

Impact of cooking on the sensory perception and volatile compounds of *Takifugu rubripes*

Danni Zhang ^a, Ni Yang ^b, Ian D. Fisk ^{b,c}, Jintao Li ^a, Yuan Liu ^{a,*}, Wenli Wang ^{a,**}

^a Department of Food Science & Technology, School of Agriculture & Biology, Shanghai Jiao Tong University, Shanghai 200240, China

^b Division of Food, Nutrition and Dietetics, School of Biosciences, University of Nottingham, Sutton Bonington Campus, Loughborough LE12 5RD, UK

^c University of Adelaide, North Terrace, Adelaide SA 5005, Australia

* Corresponding author.

Email Addresses: *y_liu@sjtu.edu.cn (Yuan Liu), **wenli-wang@sjtu.edu.cn (Wenli Wang)

1 **Abstract**

2 *Takifugu rubripes* is well-known for the unique flavour but can also develop a putrid off-note. To
3 eliminate off-note and promote desirable flavour, four cooking processes (boiling, steaming, microwave-
4 heating and roasting) were explored to determine their effects on cooked *T. rubripes*. The temperature
5 and water dynamics, physico-chemical properties were analysed and correlated with sensory qualities.
6 The changes of centre temperature dynamics during cooking decreased the water mobility and led to
7 varied sensory properties. Six out of ten orthonasal aroma attributes and four out of five mouthfeel
8 attributes were significantly different among samples ($p < 0.05$). Based on Partial Least Squares
9 Regression analysis, orthonasal aroma attributes “roasted” and “earthy/putrid fish” highly correlated with
10 the volatile compounds generated from Maillard reaction and lipid oxidation, respectively; meanwhile
11 mouthfeel attributes of chewy/fibre and tender/juicy were highly associated with water loss and moisture,
12 respectively. This study provides insights for optimising cooking conditions to create desirable fish
13 flavour.

14

15 **Keywords**

16 *Takifugu rubripes*, thermal cooking process, sensory, off-note, aroma

17 **1. Introduction**

18 Pufferfish (*Tetraodontidae*), a family of marine and freshwater fish belonging to *Tetraodontiformes*, is
19 well-known for its frightening toxicity all over the world. However, it has been of interest for thousands
20 of years in China, and more recently in other Eastern Asia countries including Japan and the Republic of
21 Korea due to its unique flavour (Zhou & Wang, 2017). *Takifugu rubripes* and *Takifugu obscurus* (the
22 genera of *Takifugu*), are the only two species of pufferfish that can be cultivated and processed legally in
23 China since 2016, and have been reported as a good source of protein with high nutritional qualities (Tao,
24 et al., 2012). According to Global Statistical Collections statistics from the Food and Agriculture
25 Organization of the United Nations (FAO), 69% of global production and 90% of global aquaculture
26 production occurred in China (2018), and overall production continues to increase (FAO Fisheries and
27 Aquaculture Department, 2020). *T. rubripes* is the main species to be exported in the form of fresh fish
28 or chilled fish (FAO Fisheries and Aquaculture Department, 2020). However, the fresh or chilled
29 pufferfish is extremely prone to become putrid and can develop a rancid off-flavour if not consumed or
30 stored properly. This is a concerning factor for consumers and limits the expansion of the pufferfish
31 industry.

32 Flavour is one of the important aspects of food quality. Overall, flavour perception is formed and
33 processed by the brain through a series of multiple sensory inputs. These include volatile aroma
34 compounds and non-volatile taste compounds delivered during olfaction and gustation (Reineccius,
35 2006). Ultimately, food flavour plays an important role in consumers' acceptance. For example, the
36 Equivalent Umami Concentration (EUC), calculated by umami amino acids and the 5'-nucleotides, was
37 positively related to the fish acceptability (Zhang et al., 2019). Meanwhile, slight changes in fish odour
38 were shown to have a great effect on consumer's hedonic responses (Alexi et al., 2018). There are various
39 factors influencing the flavour of fish products, such as the thermal cooking process, food ingredients,
40 *etc.*, of which the thermal cooking process is the first complex factor to be considered. The cooking
41 process can affect the fish aroma and taste by different mechanisms, such as Maillard reaction, lipid
42 oxidation, protein degradation, *etc.* (Reineccius, 2006). Additionally, thermal cooking processing reduces
43 water content and affects protein structure which will also result in different texture properties (Sun et

44 al., 2020). Therefore, it can be proposed that the appropriate cooking process may help to eliminate off-
45 flavours and be used to design different flavour profiles with different sensory qualities.

46 Recent research on pufferfish flavour mainly focused on the taste-active compounds investigation (Zhang
47 et al., 2019) and umami characterization (Wang et al., 2021) using chemical analysis and sensory
48 evaluation. However, the overall sensory properties of cooked pufferfish have never been determined.
49 Since off-flavour has always been a concerning problem for pufferfish and the thermal cooking process
50 is known to dramatically change the flavour profile, it is useful to conduct the sensory properties
51 evaluation and correlate this with the instrumental flavour analysis in order to investigate the thermal
52 processing impacts on pufferfish flavours.

53 Therefore, our hypothesis in this study is that the thermal cooking process can be used to create desirable
54 sensory qualities and mask/decrease any potential off-flavour of pufferfish which is naturally formed
55 through oxidation. The objectives of our study were (i) to establish four thermal process methods (boiling,
56 steaming, microwave-heating and roasting) and monitor the dynamic changes of temperature and water
57 during different cooking processes; (ii) to create and evaluate holistic flavour profiles of cooked
58 pufferfish by sensory evaluation (Quantitative Descriptive Analysis, QDA) and flavour analysis
59 (Electronic nose, E-nose; Gas Chromatography-Time-of-Flight -Mass Spectrometer, GC-TOF-MS); (iii)
60 to correlate sensory attributes with instrumental data by statistical analysis (Principal Component
61 Analysis, PCA; Partial Least Squares Regression, PLS-R and Hierarchical Cluster Analysis Heatmap,
62 HCA heatmap). Achieving these three objectives would generate new knowledge on how thermal
63 processes affect pufferfish flavours, and which method would be the optimum way to improve the flavour
64 profiles of cooked pufferfish, which will directly benefit the expansion and standardization of the
65 pufferfish industry.

66

67 **2. Material and Methods**

68 **2.1 Materials and reagents**

69 The dorsal muscle of *T. rubripes* fillets was purchased from Dalian Tianzheng Industrial Co., Ltd.
70 (Liaoning Province, China). Two-year-old farmed *T. rubripes* was slaughtered according to the

71 National Standard (GB/T 27624-2011) by the company. After slaughter, the dorsal muscle of fish flesh
72 (fillet) was cut off, packaged, and transported to our lab within 12 hours covered with ice, and frozen in
73 -80 °C freezer until use.

74 2,4,6-Trimethylpyridine (purity 98%, Ark Pharm, Chicago, USA) was dissolved in methanol
75 (purity ≥ 99.9%, GC standard, Aladdin®, Shanghai, China). C7-C40 Saturated alkanes dissolved in
76 hexane were purchased from Sigma-Aldrich Trading Co., Ltd. (Shanghai, China).

77 **2.2 Preparation of cooked *T. rubripes***

78 Fillets with similar thickness were thawed in a 4 °C fridge overnight. Before cooking, they were cut
79 into a similar weight (69 ± 4.00 g, 13.7 ± 0.3 cm length, 4.2 ± 0.4 cm width) from the same part. The
80 cooking time for each processing method was defined as the best time when the most pleasant fish
81 aroma was generated. The best time was determined with four specialised sensory assessors in the
82 preliminary experiment by smelling the cooked pufferfish sample with different cooking times. The
83 standardised method for each thermal process was listed below:

84 *Boiled T. rubripes (BTR)*: fillets were boiled in the boiled water at a ratio of 1:4 (fish/water, w/w) for
85 10 min without a lid.

86 *Steamed T. rubripes (STR)*: fillets were placed in a glass plate over the boiled water at a ratio of 1:10
87 (fish/water, w/w) for 25 min with a lid.

88 *Microwave-heated T. rubripes (MTR)*: fillets were covered with the baking paper, and cooked for 3.0
89 min in the 700 W microwave oven (EM7KCGWt3-NR, Midea, Guangdong Province, China).

90 *Roasted T. rubripes (RTR)*: fillets were covered with the baking paper, and roasted at 200 °C for 20 min
91 on each side in a baking oven (K42, Galanz, Guangdong Province, China).

92 Four fillets were chosen randomly for each cooking process as replicates. During cooking, the centre
93 temperature of each fillet was detected by a K/J dual input thermometer (UT320D, UNI-Trend,
94 Guangdong Province, China) to guarantee the consistent cooking process. After cooking, each fillet
95 was cooled at room temperature and weighed to calculate the remaining weight % (the weight after
96 cooking divided by the weight before cooking $\times 100\%$) and water loss % (100% minus the remaining
97 weight %).

98 Three sections of each fillet were used for different types of analysis (**Fig. S1**): 15% of the fillet was
99 used for colour and moisture analysis (labelled as part A); 50% at the middle section of the fillet was
100 used for aroma analysis (part B); rest 35% of the fillet was used for water distribution analysis (part C).

101 **2.3 Colour and water content**

102 Colour analysis was conducted on the surface of part A (**Fig. S1**) firstly after cooking. Eight replicates
103 were performed for each cooking process (2 replicates per fillet). L^* , a^* and b^* values were detected
104 with CIE1931 standard colourimetric system by the high-quality portable colourimeter (XD-1055,
105 Modern instruments, Shanghai, China), and represented the lightness, green/red and blue/yellow
106 respectively. The total colour difference (ΔE) was calculated by the following equation compared with
107 the colour of the raw fillet as the control.

$$108 \quad \Delta E = \sqrt{\Delta L^2 + \Delta a^2 + \Delta b^2}$$

109 After the colour analysis, the part A of the fillet was ground with a mortar for 1 min to analyse water
110 content following the National Standard (GB 5009.3-2016). Eight replicates were performed for each
111 cooking process (2 replicates per fillet).

112 **2.4 Low-field nuclear magnetic resonance (LF ^1H NMR)**

113 One gram sample from part C of **Fig. S1** was taken to perform LF ^1H NMR (MesoMR23-060H-I,
114 Niumag, Jiangsu Province, China) measurements at 32 °C with a 60 mm diameter probe coil. The
115 magnetic field strength and proton resonance frequency were 0.5 T and 21 MHz, respectively. The T_2
116 transverse relaxation time was acquired by Carr-Purcell-Meilboom-Gill (CPMG) sequence with the 90°
117 pulses of 12 μs and 180° pulses of 23 μs . Decay signals were collected with 0.5 ms echo time, 1000
118 echoes and 8 scan numbers. The decay curves were obtained by the instrument software (Version 2.0,
119 Niumag, Jiangsu Province, China), and multi-exponential fitted by the simultaneous iterative
120 reconstruction technique (SIRT) algorithm. Four replicates were performed for each cooking process.

121 **2.5 Electronic nose (E-nose) analysis**

122 Part B in **Fig. S1** of each fillet was ground with cooled mortars for 1 min. Two grams of each sample
123 were weighed into a 40 mL headspace vial and equilibrated at 50 °C for 20 min. After that, the sensor
124 array unit equipped with 14 metal-oxide semiconductors (MOS) sensors were exposed to the headspace

125 of samples for 60 s at an air flow rate of 1 L/min. Between samples, the system was cleaned for 60 s
126 twice at the same air flow rate. The signal of each sensor was recorded by the Software
127 (BosinTechNose, Shanghai, China), of which the maximum values of response curves were selected to
128 perform data analysis. Twelve replicates were carried out for each cooking process (3 replicates per
129 fillet).

130 **2.6 Solid-Phase Microextraction (SPME) and Gas Chromatograph-Time-of-Flight** 131 **Mass Spectrometer (GC-TOFMS)**

132 Three grams of ground fish from Section 2.5 were weighed in a 20 mL headspace vial, cooled down by
133 liquid nitrogen immediately, and stored in -80 °C freezer until GC-MS analysis. Before analysis, 10 μ L
134 internal standard (IS) of 2,4,6-trimethylpyridine (6.8 mg/L) was added into the sample vial. Each vial
135 was capped and defrosted at room temperature for 1 h. The analysis condition of SPME-GC-MS has
136 been optimised and performed as the following steps: samples were incubated at 50 °C for 20 min, and
137 volatile compounds in the headspace were extracted by a 2 cm 50/30 μ m DVB/CAR/PDMS fibre
138 (Supelco, Sigma-Aldrich, Shanghai, China) at the same temperature for 40 min. The extracted volatile
139 compounds were desorbed in the GC (7890B, Agilent, Beijing, China) inlet at 250 °C for 6 s with a
140 spitless mode, and isolated by a TG-Wax MS column (30 m length, 0.25 mm diameter, 0.25 mm
141 thickness, Thermo, Shanghai, China) with a Helium carrier flow rate of 1 mL/min. The oven
142 temperature started from 30 °C, then increased to 250 °C at a rate of 5 °C/min and held for 3 min. The
143 isolated volatile compounds were then transferred to TOF-MS (LECO, Shanghai, China) to be
144 identified with EI ionisation mode. The temperatures of the transfer line and ion source were set as
145 250 °C and 200 °C respectively. The full scan was 35-500 m/z with an acquisition rate of 10 spectra/s.
146 All samples were analysed in randomised orders. Four replicates were performed for each cooking
147 process.

148 The identification of volatile compounds was tentatively determined by comparing MS spectra with the
149 NIST 17 standard reference database (NIST 17 and Version 2.3) and then confirmed from the retention
150 index (Van Den Dool & Kratz, 1963) calculated by C7-C40 saturated alkanes under the same GC-TOF-
151 MS conditions. The semi-quantification analysis of the relative headspace concentration above each

152 sample was calculated by comparing the ratio of the peak area between the compound of interest and
153 IS, and then multiplied the concentration of the IS.

154 The relative concentration of volatile compounds ($\mu\text{g}/\text{kg}$)

$$155 = \frac{\text{Peak area of the volatile compound}}{\text{Peak area of the internal standard}} \times \frac{\text{Amount of the internal standard } (\mu\text{g})}{\text{Amount of the sample (kg)}}$$

156 **2.7 Sensory evaluation**

157 A quantitative descriptive analysis (QDA) approach was conducted in the standard sensory room (ISO
158 8589: 2007). Twelve Chinese panellists (four males and eight females, ages 22 to 30 years old) were
159 recruited who had the sensory evaluation experience of 6 months to 3 years. They were trained by four
160 sessions. The first two sessions were carried out to develop vocabularies and reach an agreement on 22
161 verbal descriptors (**Table S1**). Then, two training sessions were performed to let panellists familiarise
162 scoring scales and sample attributes according to the references shown in **Table S1**. The consensus
163 vocabularies included 10 orthonasal aroma attributes, 10 retronasal aroma attributes, 6 taste attributes, 5
164 mouthfeel attributes and 9 after-effect attributes, of which after-affect contained the modalities within
165 the aroma, taste and mouthfeel after swallowing samples.

166 Before each session, *T. rubripes* were cooked on the same day as described in Section 2.2, and 5 g
167 samples were stored in sensory sampling cups with lids at 50 °C and presented to panellists within one
168 hour. Each sampling cup was labelled with three-digit codes and served in randomised orders. During
169 each session, the orthonasal aroma attributes were scored firstly by smelling samples, while retronasal
170 aroma, taste and mouthfeel attributes were scored when chewing samples, and after-affect attributes were
171 scored after swallowing samples in the end. Three repeated sessions were held for scoring samples using
172 a continuously unstructured line scale anchored 0 (left, no perception) to 15 (right, extremely strong
173 perception) as three replicates.

174 **2.8 Statistical analysis**

175 Data were analysed by the Analysis of Variance (ANOVA) using IBM SPSS Statistics software
176 (Version 20) with a Post-hoc Tukey's test at $\alpha=0.05$. Principal Component Analysis (PCA), Partial
177 Least Squares Regression (PLS-R) and Hierarchical Cluster Analysis Heatmap (HCA heatmap)
178 analysis were achieved by XLSTAT (Annual Version 2020.1.3, Addinsoft Inc.).

180 **3. Results and Discussion**

181 **3.1 Centre temperature changes during cooking *T. rubripes***

182 Diverse temperature evolutions on fish during different thermal cooking processes would result in the
183 distinct physico-chemical and sensory properties of cooked fish. So the centre temperature curves of
184 different cooked *T. rubripes* were monitored and shown in **Fig. 1A**. All centre temperatures increased
185 to near 100 °C, but microwave-heated *T. rubripes* (MTR) took the shortest time (less than 2.5 min) to
186 reach over 90 °C. By contrast, roasted *T. rubripes* (RTR) spent the longest time (more than 10 min)
187 reaching over 90 °C and held for the longest time (25 min) over 90 °C, when compared with those of
188 boiled *T. rubripes* (BTR, 0 min over 90 °C), steamed *T. rubripes* (STR, 10 min over 90 °C) and
189 microwave-heated *T. rubripes* (MTR, 0.5 min over 90 °C).

190 The microwave-heating process can be the most efficient way to cook food because it penetrates
191 energy into foods by the heat radiation, which converses electromagnetic energy to thermal energy as a
192 result of dipole and ion mechanism (Chandrasekaran, Ramanathan, & Basak, 2013). However, for
193 traditional cooking processes (boiling, steaming and roasting), heat is transferred to the surface of food
194 by the heat convection, and the approximate values of convective heat transfer coefficients were
195 reported as 20-100 (air), 3 000-100 000 (boiling water), 5 000-100 000 (steamed water) for respective
196 free convection (Hanson, 1990). This is consistent with the results on the heating rate of different
197 cooking processes observed in this study, which indicated that the air convection would be the least
198 efficient (i.e., RTR) followed by boiling water (i.e., BTR) and steamed water (i.e., STR). Apart from
199 the heat efficiency, heating time is another variable need to be considered. Increasing the reaction time
200 may not necessarily increase flavour intensity but influence the flavour balance (Reineccius, 2006).
201 Until now, more research has worked on aroma changes from Maillard reactions over time, while very
202 few researches on taste compounds change over time. For example, the kinetic modelling in the potato
203 model system demonstrated that Strecker aldehyde levels decreased on prolonged heating while
204 alkylpyrazine levels increased (Low, Mottram, & Elmore, 2006). This would result in different sensory
205 perception and aroma profiles, which will be discussed in the following sections.

206 **3.2 Water dynamics of cooked *T. rubripes***

207 With the increase of temperature, water mobility and distribution may change during thermal cooking
208 processes, leading to different sensory qualities. The water mobility reflects the binding relationship
209 between water and protein in the meat system (Zhou et al., 2019). The results of using LF-NMR to
210 compare the water dynamics of raw fish and four types of thermally processed fish were shown in **Fig.**
211 **1B**. Three main “peaks” were detected in the range of 0-10 ms, 10-100 ms and 100-1000 ms, which
212 represented bound water (T_{21}) associated with macromolecules tightly, immobilized water (T_{22}) located
213 within the highly organised protein structures, and free water (T_{23}) reflected the extra-myofibrillar water,
214 respectively (Bertram et al., 2001). Compared with RawTR, cooking processes caused the curve shift
215 toward lower relaxation time visually (**Fig. 1B**), which is consistent with the previous report (Sun et al.,
216 2020). The protons with lower relaxation time indicated that the cooking process in this study reduced
217 the water mobility and increased the binding between water and protein backbone. This result is more
218 evident in **Fig. 1C** and **Table S2**, because T_{22} and T_{23} of all cooked samples were lower than raw *T.*
219 *rubripes* (RawTR) significantly, which indicated a significant lower transverse relaxation time of protein-
220 binding water and free water in all cooked samples ($p < 0.05$). During the cooking process, the fibre
221 bundles network was destroyed (Cao et al., 2018), thereby, the immobilised water was transformed into
222 free water firstly and evaporated from the fish system. So, the remaining protons were restrained in the
223 fish system leading to decreased mobility (Sun et al., 2020). Comparing with different thermal processing
224 methods, roasting (RTR) resulted in the lowest T_{22} and T_{23} values, which indicated the most significant
225 reduction in transverse relaxation time ($p < 0.05$) linking with reduced water mobility.

226 Additionally, the changes in the amplitude of peak area proportion at three defined intervals (T_{21} , T_{22} ,
227 T_{23}) were summarised in **Fig. 1D** and **Table S2**. The results of P_{21} , P_{22} and P_{23} corresponded to the ratio
228 of bound water, immobilised water and free water, respectively. Despite the sample type, P_{21} counted for
229 3-8%, P_{22} generally had 88-92%, and the rest of 1-7% was P_{23} . Compared with RawTR, cooking
230 processes led to the increase in P_{21} of all cooked samples, particularly, P_{21} of STR, MTR and RTR were
231 significantly different from RawTR ($p < 0.05$). So the proportion of bound water increased significantly
232 ($p < 0.05$) in most cooked fish samples except BTR. However, there was no significant difference between

233 all samples in their P_{22} values. Regarding P_{23} results, only RTR had a significantly different proportion
234 ($p<0.05$), comparing with other cooked samples and RawTR, so apart from roasting, other cooking
235 methods did not significantly change the free water proportion to its original level. Multiple factors of
236 cooking processes would influence the water dynamic, such as the availability of water, heating
237 efficiency or heating time. The partition between water and fish may be easier to reach equilibrium for
238 BTR, leading to the least changes of all relaxation time and proportions values (more similar water
239 dynamics) between BTR and RawTR, while by contrast, it would be harder to achieve balance in MTR
240 and RTR systems. However, it was observed that there was no significant difference between MTR and
241 RTR in terms of all three relaxation times (T_{21} , T_{22} , T_{23}), P_{21} and P_{22} values, which may be caused by the
242 microwave to break hydrogen bonds between water and other macromolecules in an efficiency way (Cao
243 et al., 2018). However, there was not enough time for free water to evaporate from the MTR system,
244 leading to a similar P_{23} value between MTR and RTR.

245 **3.3 Water content and colour of cooked *T. rubripes***

246 Different in the centre temperature and water dynamics led to diverse physical-chemical properties, so
247 the remaining weight, moisture content and colour were measured (**Table 1**). Comparing the remaining
248 weight of cooked samples, BTR had around 68% remaining weight, which is the significantly highest
249 level ($p<0.05$). Both STR and MTR had around 63% remaining weight, and RTR had the lowest level
250 around 48% which is significantly different from other samples ($p<0.05$). Similarly, RTR had a
251 significantly lower moisture content (57%), which is around 23% lower than its level in RawTR (80%).
252 MTR, STR and BTR had 69-70% moisture content, which is 10-11% significantly lower than RawTR
253 ($p<0.05$). So moisture content reduced significantly for all four types of thermal processing, but the
254 roasting process resulted in the lowest moisture content with the lowest remaining weight, while no
255 significant difference between STR and MTR. BTR was cooked in boiling water, as a result of the
256 highest value of remaining weight and moisture. Compared with MTR, STR was cooked under the
257 steam of boiling water for a longer time, while the more efficient heat transfer for MTR could
258 transform more immobilised water into free water without enough time to evaporate, leading to no
259 significant difference between them.

260 By comparison of colour results, RTR had the significantly highest a^* and b^* values ($p < 0.05$) among
261 raw and cooked samples, so RTR was significantly more red and yellow. The lightness of raw fish (L^*)
262 increased with cooking significantly ($p < 0.05$), and comparing with microwave-heating (MTR) with the
263 largest increase, RTR had the least increase. The total colour difference (ΔE) of all cooked samples
264 were calculated based on RawTR data, and their values were similar at 26-28. The colour difference of
265 ΔE ($\Delta E \geq 2.2 \pm 1.3$) corresponded to a Just Noticeable Difference by human eyes (Mahy, Van Eycken, &
266 Oosterlinck, 1994), so the colour difference between raw fish and cooked fish was perceptible by
267 human eyes. As for RTR, a long heating time at high temperature resulted in the brown colour
268 indicating the most intense Maillard reaction, which is the basis for flavour generation in thermal
269 cooking foods, especially some meaty and savour flavour compounds (Parker, Elmore, & Methven,
270 2015). Colour can influence flavour perception matched with the major components of flavour
271 (olfactory, gustatory and trigeminal sensations) (Bordiga & Nollet, 2019). But previous research (Alexi
272 et al., 2018) indicated that the consumer's hedonic responses for cooked fish were more related to
273 texture and odour/flavour rather than colour. Therefore, the main focus of later sensory evaluation was
274 the flavour and texture of cooked pufferfish samples.

275 **3.4 Perceived sensory attributes of cooked *T. rubripes***

276 Quantitative descriptive analysis (QDA) was carried out to evaluate the overall sensory profiles of
277 cooked *T. rubripes* and to investigate any perceived differences affected by cooking processes. The
278 sensory quality was defined to measure the orthonasal/retronasal aroma (O/R), taste (T), mouthfeel (M)
279 and after-effect (A) perception. Generally, a total of 40 attributes (22 descriptors, **Table S2**) were selected,
280 including 20 for O/R, 6 for T, 5 for M and 9 for A, and their perceived intensities were calculated (**Fig.**
281 **2** and **Table S3**). Among four cooked samples, 16 sensory attributes had significantly different intensities
282 ($p < 0.05$), including most of the oronasal and mouthfeel attributes. Among all 40 perceived attributes, the
283 intensities of fishy-O/R and umami-A attributes were at the highest concentrations for all cooked samples
284 (intensities higher than 8.0), which indicated that fishy and umami could be two prominent sensory
285 attributes in this study. Among four cooked samples, RTR had significantly the highest intensities of
286 roasted-O/R, oily-O/R, bitter-T, salty-T, fibre-T, chewy-T, sour-A and astringent-A attributes, and

287 significantly the lowest scores for the putrid fish-O, earthy-O, soybean-O, dairy-O, juicy-M and tender-
288 M ($p < 0.05$). However, these attributes did not change significantly among the other three cooked samples
289 (BTR, STR and MTR), except for the highest intensity of juicy-M attribute for MTR.

290 Cooking processes affect the sensory quality. Previous studies proved that similar aroma, taste, flavour
291 and texture profiles were obtained under similar cooking methods (steaming at 100 °C for 20 min and
292 roasting at 180 °C for 15 min) (Alexi et al., 2019). In this study, four cooking processes varied a lot,
293 resulting in various sensory qualities. Orthonasal aroma is associated with key aroma-active compounds
294 such as those generated from Maillard reaction, lipid oxidation, *etc.* (Reineccius, 2006), which are
295 delivered to the nose during inhalation directly from the product without consumption, while the
296 retronasal aroma relates to aroma compounds that are delivered to the nasal cavity during chewing and/or
297 swallowing. Comparing orthonasal aroma with retronasal aroma, most aroma attributes (e.g., fishy,
298 roasted, boiled potato, boiled mushroom, boiled vegetable) had no significant difference in their
299 perceived intensities of the same cooked pufferfish sample, which was consistent with the previous report
300 (Du et al., 2020). Taste attributes are associated with key tastants generated from protein degradation,
301 Maillard reaction *etc.* (Reineccius, 2006). Umami, the highest taste intensities characteristic in all cooked
302 samples, is considered as a kind of typical taste characteristic for fish and can interact with other taste
303 substances resulting in the overall taste perception (Wang, Zhou, & Liu, 2020). RTR was perceived as
304 having the significantly highest saltiness and bitterness ($p < 0.05$), this was perhaps due to a more intense
305 Maillard chemistry reaction, resulting in the formation of more Maillard chemistry biproducts and a
306 lower moisture content thereby increasing the relative concentration. Besides, salty perception also can
307 be enhanced by umami substances (Wang, Zhou, & Liu, 2020) or salt-related odours (Thomas-Danguin
308 et al., 2019). Furthermore, four mouthfeel attributes exhibited significant difference ($p < 0.05$), except for
309 “crumbly”, indicating their importance on the overall sensory profiles, which was also highlighted by
310 previous research on the consumers’ hedonic responses to fish species (Alexi et al., 2018).

311 **3.5 Orthonasal volatile compounds analysis of cooked *T. rubripes***

312 Considering that most of the orthonasal sensory attributes differed significantly among cooked samples
313 ($p < 0.05$) (Fig. 2), orthonasal volatile compounds were further analysed by E-nose and GC-TOF-MS.

314 **3.5.1 Dynamic aroma profile changes of cooked *T. rubripes***

315 As a quick analytical tool to compare with the sensory analysis, E-nose was applied to rapidly detect
316 aroma profiles of cooked *T. rubripes*. The E-nose results of the maximal corresponding signal values of
317 sensors were summarised in a radar chart (**Fig. 3A**) and a PCA graph (**Fig. 3B**). **Fig. 3A** described the
318 response signal of each sensor corresponded to every cooked sample, and statistical results indicated that
319 all the sensors detected a significant difference among the samples ($p < 0.05$). This result indicated the
320 good sensitivity and specificity of MOS sensors, which matched with previous report (Jiang & Liu, 2020).
321 Different sensors could be more sensitive to a specific product, for example, Sensor_1 and Sensor_9
322 showed their better sensitivity to RTR, and other sensors (Sensor_11, Sensor_12 and Sensor_13) were
323 more sensitive to RawTR/MTR. MOS sensors are widely used in the application of food detection
324 compared with biosensors because of their good performance in complicated food matrices (Jiang & Liu,
325 2020). Further studies are required to investigate the sensitivity of the MOS sensors for specific groups
326 of aroma compounds.

327 On the other hand, data from MOS sensors provided some fingerprints to demonstrate the aroma profile
328 differences between cooked pufferfish samples. As shown in the PCA plot (**Fig. 3B**), the first two
329 principal components - PC1 and PC2 explained 48.78% and 41.22% of the variance respectively.
330 Different cooked samples were clustered into different groups: the location of different samples evolved
331 from RawRT at the upper left corner to other cooked samples (MTR, BTR and STR) and RTR samples
332 spread across the 4th quadrant of the PCA. This changing trend indicated that RTR had a distinct aroma
333 profile than RawRT, and the aroma profiles of BTR and STR were more similar, while MTR aroma
334 profiles were the closest one to RawRT. The E-nose technique combined with the data processing method
335 could demonstrate the dynamic change of overall aroma profiles of cooked pufferfish, as well as other
336 aquatic products like the cold-smoked Spanish mackerel (Huang et al., 2019). It could be a powerful tool
337 for rapidly evaluating and monitoring the food aroma changes (Jiang & Liu, 2020).

338 **3.5.2 Orthonasal volatile compounds of cooked *T. rubripes***

339 Since E-nose could not reveal the change of each volatile compound of cooked *T. rubripes*, SPME-GC-
340 TOFMS was applied to identify and quantify the relevant volatile compounds. A total of 117 volatile

341 compounds were identified in cooked samples, including 36 hydrocarbons, 11 sulphur-containing
342 compounds, 15 nitrogen-containing compounds, 12 aldehydes, 15 ketones, 18 alcohols and 10
343 compounds from other chemical families (**Table 2**). Comparing the total number of volatiles detected in
344 different samples, RawTR had the lowest total number (83), and RTR had the largest total number (117),
345 whilst the total number for BTR (94), STR (100) and MTR (98) were in the middle range. The odorants'
346 compositions among BTR, STR and MTR were similar, but their concentrations differed for specific
347 compounds. Despite the number of hydrocarbons accounted for 30% of the total number of volatile
348 compounds (**Table 2**), most of their thresholds are normally high (Shahidi, 1998), so they might not make
349 a great contribution to the overall fish aroma.

350 Among all sulphur-containing compounds (2 thiols, 1 thial, 2 alkyl sulfides, 2 thiophene and 3 thiazoles),
351 almost no sulphur-containing compounds could be detected in RawTR, while all 11 sulphur-containing
352 compounds were detected in RTR, and most of their concentrations were the highest in RTR significantly
353 ($p < 0.05$). Additionally, comparing with other cooked samples, RTR had all 15 nitrogen-containing
354 compounds detected (1 amine, 1 pyridine, 1 pyrrole and 12 pyrazines), and all of them were at the
355 significantly highest levels ($p < 0.05$). The reason could be that these heterocyclic compounds are formed
356 through the Maillard reaction (Parker et al., 2015; Reineccius, 2006), so almost none of the heterocyclic
357 compounds were found in RawTR, and the longest heating time in the RTR system led to more
358 heterocyclic compounds generated (such as the presence of methional and much higher level of
359 methanethiol). However, dimethyl disulphide and dimethyl trisulphide showed different trends (STR had
360 a higher level than RTR). Dimethyl disulfide and dimethyl trisulfide are secondary volatiles generated
361 from methanethiol, a product from methional (Strecker aldehydes) which was originally from methionine
362 by Strecker degradation (Schlüter et al., 1999). Different heating methods would result in their varying
363 levels, and one of the reasons could be different physical and chemical interactions between sulphur-
364 containing compounds and proteins in foods during thermal processing. Moreover, trimethylamine
365 (TMA) was also detected in raw fish because it can be generated by trimethylamine oxide (TMAO), a
366 product from soluble sarcoplasmic proteins and nucleotides during alterations of fish post-mortem
367 (Bordiga & Nollet, 2019). It has been reported that the formation of TMA increased as cooking time
368 prolonged (Hughes, 1959), which matched the results of our study that RTR had the highest level.

369 Although TMA was often regarded as “off-note and fishy” for fish aroma (Shahidi, 1998), it should be
370 considered as an essential important compound that contributes to the aroma of delicious prawn meat
371 (Mall & Schieberle, 2017).

372 Among 12 aldehydes detected in the samples, 2-methylbutanal and 3-methylbutanal along with furfural
373 and benzaldehyde were the only 4 aldehydes with the significantly highest concentration in RTR ($p < 0.05$).
374 However, except nonanal, the concentrations of other aldehydes were the lowest in RTR, despite no
375 significant difference among the other three cooked samples. The first 4 aldehydes mentioned above
376 were generated from Strecker degradation or Maillard reaction, and other aldehydes were generated from
377 lipid oxidation (Shahidi, 1998; Yang et al., 2017). Therefore, the roasting process in our study resulted
378 in the most intense Maillard reaction and generated a higher level of specific aldehydes. Similarly, among
379 all 15 ketones in cooked samples, RTR had the significantly highest concentrations ($p < 0.05$) of 2
380 furanones, 4 hydroxyketones and 1 lactone, which were products of the Maillard reaction. Other ketones
381 were almost generated from lipid oxidation (Shahidi, 1998; Yang et al., 2017), so the concentration of
382 these ketones (methyl ketones, 2,3-pentanedione and 3,5-octadienone) showed different patterns. Diones
383 have been reported to be generated by lipid oxidation and further involved in the Strecker degradation
384 and Maillard reaction to form heterocyclic compounds, such as pyrazines and thiazoles (Parker, Elmore,
385 & Methven, 2015), so 2,3-pentanedione may be generated and participated in other chemical reactions
386 during the roasted process leading to the decrease of its concentration in RTR.

387 Alcohols, derived from lipid oxidation, are considered to contribute to the fresh fish aroma, whereas their
388 contributions are less important due to their high threshold values compared with carbonyl compounds
389 (Shahidi, 1998). Among all cooked samples for all 18 alcohols detected, the concentrations of 15 alcohols
390 were the highest in MTR, which indicated that the more intense lipid oxidation happened in the
391 microwave-heating system. Although microwave-heating is the most efficient way to cook fish, non-
392 uniform temperature distribution may lead to cold and hot spots, therefore, enzymes in the cold spot
393 might continue accumulating the lipid oxidation (Parker, Elmore, & Methven, 2015). Besides, there were
394 3 esters, 4 furans and 3 acids identified in cooked fish. RTR had the highest level for most esters and
395 furans and the cooked fish samples had a lower level of acids than raw samples.

396 To visualize the correlations of mass aroma data, Principal Component Analysis (PCA) was applied to

397 extract information from 15 important volatile compounds with relative OAVs higher than 1 (**Fig. 3C**).
398 The two principal components (PCs) explained 92.00% of the variance, representing the good separation
399 for all samples. RTR and Raw TR were located far from each other, while BTR, MTR and STR were
400 close to each other, whose trend was consistent with PCA from data of E-nose (**Fig. 3B**). BTR, MTR and
401 STR were clustered on the positive side of the PC1 axis, while MTR/STR and BTR were located on the
402 positive and negative of the PC2 axis respectively. Meanwhile, BTR and RawTR were on the negative
403 of PC1, of which RTR and RawTR were separately clustered on the positive and negative of PC2
404 respectively. As shown in **Fig. 3C**, there were 7 aldehydes, 1 ketone and 2 alcohols with relative OAVs
405 higher than 1, of which only 2-methylbutanal and 3-methylbutanal were closely correlated with RTR
406 (**Fig. 3C**) because of their generations from Strecker degradation. In addition, 2 sulphur-containing
407 compounds (methanethiol and trimethylamine) and both nitrogen-containing compounds (2-ethyl-3,5-
408 dimethylpyrazine and 2-furfurylthiol) were closely correlated with RTR, while another sulphur-
409 containing compound (dimethyl trisulfide) was more related with STR, which was convinced by their
410 concentrations in **Table 2**. Heterocyclic compounds normally play a key role in the meat aroma with low
411 thresholds (Shahidi, 1998), and most of these compounds were generated from Strecker degradation and
412 Maillard reaction, so the cooking process with higher temperature, less water content and longer heating
413 time, would be a good way to drive the pleasant aroma generation.

414 **3.6 Correlation between orthonasal volatile compounds and sensory aroma** 415 **attributes**

416 Cooking processes can modify food aroma by various chemical reactions, which has been demonstrated
417 by the individual results from sensory analysis and instrumental analysis in this study. To investigate the
418 correlations between them, Partial Least Squares Regression (PLS-R) analysis was performed based on
419 the scores of sensory orthonasal attributes (**Fig. 2** and **Table S3**) and the concentrations of volatile
420 compounds (**Table 2**) as Y quantitative dependent variables and X quantitative explanatory variables,
421 respectively. BTR, STR, MTR and RTR were set as different observation labels and four components
422 were set as a fixed number. As illustrated in **Fig. 4A**, the first two representative components were
423 displayed for the first two axes, and STR/MTR, BTR and RTR were projected into the 2nd, 3rd and 4th

424 quadrants, respectively. The inner circle and outer circle represent 50% and 100% of the variables'
425 explained variance, while the Q^2 , R^2Y and R^2X cumulated index were 0.846, 0.956 and 0.874 respectively.
426 Except for 3 hydrocarbons, benzothiazole and 3 alcohols, all the other Y and X variables were between
427 two circles, so this PLS-R model provided a good quality predictive model.

428 RTR was positively correlated with orthonasal “fishy, oily and roasted” sensory attributes and those
429 odorants derived from Strecker degradation or Maillard reaction, such as sulphur-containing and
430 nitrogen-containing compounds. Meanwhile, STR and MTR positively correlated with other sensory
431 attributes and odorants generated from lipid oxidation, such as most aldehydes, alcohols and some
432 ketones, while the aroma of BTR was less intense because of limited variables around it. Moreover, the
433 “fishy-O” attribute factors projected on the positive dimension of t1 axes and negatively associated with
434 the “putrid fish-O” attribute projected on the negative dimension of t1 axes. Similarly, the “oily-O and
435 roasted-O” attributes and Maillard-derived odorants negatively related to other sensory attributes (such
436 as boiled vegetable-O and earthy-O) and Lipid-oxidation-derived odorants, which deep-rooted the effect
437 of an efficient Maillard reaction on the orthonasal aroma perception and the generation of heterocyclic
438 compounds. Furthermore, the “roasted-O, oily-O and fishy-O” attributes were significantly positively
439 correlated with heterocyclic compounds, while “boiled vegetable/potato-O, earthy-O, dairy-O” attributes
440 had a significantly positive correlation with most of aldehydes and alcohols from lipid oxidation.

441 Orthonasal sensory attributes were closely correlated with detected aroma compounds. To some extent,
442 thiazoles and pyrazines can promote similar sensory properties (Reineccius, 2006), which had a
443 significant positive correlation with “roasted-O” sensory attribute. TMA (No. 48) had a significantly
444 positive association with pleasant “fishy-O” rather than unpleasant “putrid fish-O” sensory attributes,
445 imparting the positive contribution with an appropriate amount of TMA. Meanwhile, off-notes like
446 “boiled vegetable-O, earthy-O and putrid fish-O” were highly correlated with most of the aldehydes and
447 cooking processes with STR (mild temperature and abundant water) or MTR (short heating time). As for
448 the higher concentration of aldehydes correlating with off-notes, high moisture in the cooking system
449 might accelerate lipid oxidation leading to the generation of most aldehydes (Damodaran & Parkin, 2017).
450 Or, there might be an irreversible chemical reaction or reversible binding between aldehyde and protein,
451 resulting in the decrease of aldehydes’ concentrations in RTR (Reineccius, 2006; Xu et al., 2020).

452 Therefore, the cooking process with less water, higher temperature and longer heating is more likely to
453 decrease the off-notes and increase roasted pleasant notes. However, more details on the effect of cooking
454 temperature/time and water content on the generation of aroma-active compounds affected by cooking
455 processes still need to be explored by the GC- olfactometry technique.

456 **3.7 Correlation between water properties and sensory mouthfeel attributes**

457 Besides orthonasal sensory attributes, 4 out of 5 mouthfeel attributes had a significant difference ($p < 0.05$)
458 among four cooked *T. rubripes* (**Fig. 2** and **Table S3**), which were the most important attribute categories
459 to distinguish four cooked *T. rubripes*. The mouthfeel attributes correspond to the perception of texture
460 properties during chewing (Roberts & Taylor, 2000), which have been reported to correlate with water
461 properties (Sun et al., 2020). Therefore, the relationship between mouthfeel attributes (chewy, fibre,
462 tender, and juicy) and water properties (water loss, moisture content and P_{21} , P_{23} , T_{21} , T_{22} , T_{23} from LF-
463 NMR) were plotted using Hierarchical Clustering Analysis (HCA) and an associated Heatmap (**Fig. 4B**)
464 using the results with the significant difference among the cooked samples ($p < 0.05$). Data values
465 corresponded with different colours (blue to red through white) in each rectangular tiling, of which blue
466 to red colour meant the low to high abundance. The dendrogram showed that four cooked samples were
467 separated into three clusters: STR and MTR constituted the first group, which was then clustered as the
468 second group with BTR; while RTR was in an isolated third group. So comparing among different
469 thermal processing methods, the roasting process resulted in products with different water dynamics
470 (higher P_{21} , lower P_{23} , T_{22} and T_{23}) and lower moisture content with higher water loss, which led to more
471 distinct mouthfeels (more chewy and fibrous, less tender and juicy) than other three cooked samples. So,
472 as shown in the correlation between water properties and sensory attributes, two distinctive clusters were
473 identified which exhibited obvious differences amongst cooked samples. Four indexes (water loss,
474 chewy-M, fibre-M and P_{21}) comprised the upper clusters of **Fig. 4B** with the higher values in RTR.
475 Chewy-M and fibre-M attributes were more relevant with the water loss, compared with P_{21} . By contrast,
476 the other 6 indexes were clustered in another group because of lower values in RTR, demonstrating the
477 positive correlation among P_{23} , T_{22} , T_{23} , tender-M, moisture and juicy-M. Within this cluster, one small
478 cluster contained tender-M, juicy-M and moisture, reflecting their higher correlation.

479 During cooking processes, the fish protein structure denatures in many ways, such as myofibrillar
480 contraction, connective tissues solubilisation and sarcoplasmic protein aggregation (Tornberg, 2005).
481 The transversal and longitudinal shrinkage of fibres can lead to the increased width of the gap between
482 fibres and their surrounding endomysium, and the shortening of sarcomere and fibre, respectively
483 (Tornberg, 2005). As shown in the previous report (Wang et al., 2020), with the increase of the heating
484 temperature on surf clam, the myofibril stretched over to form a streak pattern, and then underwent
485 dilaceration, contraction and separated into the fragmented structure. Meanwhile, with the increase of
486 the cooking time, the gap between fibres was also more apparent under the microscope (Xia et al., 2017),
487 which was also convinced by the instrumental texture profile analysis on the hog maw that the chewiness
488 decreased apparently as cooking time prolonged (Zheng et al., 2021). Therefore, for RTR, the highest
489 temperature and longest heating time produced more fragments with less water, dominated the high
490 values and the positive correlation between chewy, fibre mouthfeel attributes and water loss. By contrast,
491 it is reported that the microwave-heating process with the faster heating rate and less heating time could
492 enhance disulphide bonds but denatured protein inadequately, which result in higher transverse relaxation
493 time values of immobilised water T_{22} and free water T_{23} , a better gel network and tenderness mouthfeel
494 (Wang et al., 2021). This corresponded to the positive correlation among T_{22} , T_{23} , tender-M, juicy-M and
495 moisture indexes for MTR.

496

497 **4. Conclusion**

498 The sensory and related physico-chemical properties of *T. rubripes* (pufferfish) were investigated when
499 four cooking processes (i.e. boiling, steaming, microwave-heating and roasting) were applied. The
500 changes of centre temperature dynamics led to different water dynamics and the decrease of the water
501 mobility during thermal cooking processes, which finally resulted in different physico-chemical
502 properties and sensory properties of cooked pufferfish. Sensory analysis generated 40 attributes (22
503 descriptors), including 20 orthonasal/retronasal aroma (O/R), 6 taste (T), 5 mouthfeel (M) and 9 after-
504 effect (A) attributes. The top two sensory properties were orthonasal aroma and mouthfeel, and it was
505 possible to differentiate the four cooked samples. The correlation of orthonasal sensory attributes with

506 volatile compounds was observed, such as “roasted-O, oily-O and fishy-O” attributes which were
507 highly related with the contribution of most heterocyclic compounds from the Maillard reaction, and
508 off-notes like “boiled vegetable-O, earthy-O and putrid fish-O” highly associated with most aldehydes
509 and alcohols derived from lipid oxidation. The specific mouthfeel attributes of chewy and fibre were
510 highly correlated with the water loss, while the tender and juicy mouthfeel attributes were highly
511 associated with moisture. The cooking process with low water content, high temperature and long
512 heating time (i.e., roasting) might be the best method, which generated pleasant roasted aromas and
513 reduced levels of off-notes with reduced tenderness and juiciness mouthfeel. Overall, the thermal
514 process is an essential step to create a desirable sensory quality of cooked pufferfish with a reduced risk
515 of rancidity compared to the raw fish, and different methods resulted in distinct flavour and texture
516 profiles. The sensory attributes showed good correlations with instrumental analysis, so the
517 instrumental data can be used as markers for the sensory quality evaluation and as tools for the
518 production chain of cooked pufferfish. The combination of sensory and analytical results proposed an
519 optimal cooking process for fish processing companies to meet consumers requirements.

520

521 **Acknowledgements**

522 This study is supported by the National Natural Science Foundation of China (Grant No. 31972198,
523 31901813). We are also grateful to the Instrumental Analysis Centre of Shanghai Jiao Tong University
524 for providing instruments.

Reference

- Alexi, N., Byrne, D. V., Nanou, E., & Grigorakis, K. (2018). Investigation of sensory profiles and hedonic drivers of emerging aquaculture fish species. *Journal of the Science of Food and Agriculture*, 98(3), 1179-1187. <https://doi.org/10.1002/jsfa.8571>.
- Alexi, N., Kogiannou, D., Oikonomopoulou, I., Kalogeropoulos, N., Byrne, D. V., & Grigorakis, K. (2019). Culinary preparation effects on lipid and sensory quality of farmed gilthead seabream (*Sparus aurata*) and meagre (*Argyrosomus regius*): An inter-species comparison. *Food Chemistry*, 301, 1252623. <https://doi.org/10.1016/j.foodchem.2019.125263>.
- Bertram, H. C., Karlsson, A. H., Rasmussen, M., Pedersen, O. D., Dønstrup, S., & Andersen, H. J. (2001). Origin of Multiexponential T_2 Relaxation in Muscle Myowater. *Journal of Agricultural and Food Chemistry*, 49(6), 3092-3100. <https://doi.org/10.1021/jf001402t>.
- Bordiga, M., & Nollet, L. M. L. (2019). *Food aroma evolution: during food processing, cooking, and aging*. (1 ed.). CRC Press (Chapter 25, Fish). <https://doi.org/10.1201/9780429441837>.
- Cao, M., Cao, A., Wang, J., Cai, L., Regenstein, J., Ruan, Y., & Li, X. (2018). Effect of magnetic nanoparticles plus microwave or far-infrared thawing on protein conformation changes and moisture migration of red seabream (*Pagrus Major*) fillets. *Food Chemistry*, 266, 498-507. <https://doi.org/10.1016/j.foodchem.2018.06.057>.
- Chandrasekaran, S., Ramanathan, S., & Basak, T. (2013). Microwave food processing—A review. *Food Research International*, 52(1), 243-261. <https://doi.org/10.1016/j.foodres.2013.02.033>.
- Damodaran, S., & Parkin, K. L. (2017). *Fennema's food chemistry*. (5 ed.). CRC press (Chapter 2, Water and ice relations in foods). <https://doi.org/10.1201/9781315372914>.
- Du, X., Sissons, J., Shanks, M., & Plotto, A. (2020). Aroma and flavor profile of raw and roasted *Agaricus bisporus* mushrooms using a panel trained with aroma chemicals. *LWT-Food Science and Technology*, 138, 110596. <https://doi.org/10.1016/j.lwt.2020.110596>.
- FAO Fisheries and Aquaculture Department (2020). Fishery Commodities Global Production and Trade (online query). Retrived on 5 November 2020 from <http://www.fao.org/fishery/statistics/global-commodities-production/query/en>.
- Hanson, R. E. (1990). Cooking technology. *43rd Reciprocal Meat Conference Proceeding*, 44, 109-115.
- Huang, X. H., Qi, L. B., Fu, B. S., Chen, Z. H., Zhang, Y. Y., Du, M., & Qin, L. (2019). Flavor formation in different production steps during the processing of cold-smoked Spanish mackerel. *Food Chemistry*, 286, 241-249. <https://doi.org/10.1016/j.foodchem.2019.01.211>.
- Hughes, R. B. (1959). Chemical studies on the herring (*Clupea Harengus*). I.—Trimethylamine oxide and volatile amines in fresh, spoiling and cooked herring flesh. *Journal of the Science of Food and Agriculture*, 10(8), 431-436. <https://doi.org/10.1002/jsfa.2740100806>.
- Jiang, S., & Liu, Y. (2020). Gas sensors for volatile compounds analysis in muscle foods: A review. *TrAC Trends in Analytical Chemistry*, 126, 115877. <https://doi.org/10.1016/j.trac.2020.115877>.
- Low, M. Y., Mottram, D. S., & Elmore, J. S. (2006). Relationship between acrylamide formation and the generation of flavour in heated foods. *Developments in Food Science*, 43, 363-366. [https://doi.org/10.1016/S0167-4501\(06\)80086-5](https://doi.org/10.1016/S0167-4501(06)80086-5).
- Mahy, M., Van Eycken, L., & Oosterlinck, A. (1994). Evaluation of uniform color spaces developed after the adoption of CIELAB and CIELUV. *COLOR research and application*, 19(2), 105-121. <https://doi.org/10.1111/j.1520-6378.1994.tb00070.x>.
- Mall, V., & Schieberle, P. (2017). Evaluation of key aroma compounds in processed prawns (whiteleg shrimp) by quantitation and aroma recombination experiments. *Journal of Agricultural and Food Chemistry*, 65(13), 2776-2783. <https://doi.org/10.1021/acs.jafc.7b00636>.
- Parker, J. K., Elmore, J. S., & Methven, L. (2015). *Flavour development, analysis and perception in food and beverages*. (1 ed.). Elsevier (Chapter 8, Thermal generation or aroma, Chapte 9, The role of sulfur chemistry in thermal generation of aroma). <https://doi.org/10.1016/C2013-0-16460-4>.
- Reineccius, G. (2006). *Flavor chemistry and technology*. (2 ed.). CRC press (Chapter 1, An overview of flavor perception, Chapter 5, Changes in food flavor due to processing, Chapter 6, Flavor release from foods). <https://doi.org/10.1201/9780203485347>.
- Roberts, D. D., & Taylor, A. J. (2000). *Flavor Release*. ACS symposium series (Chapter 3, Real-time

- flavor release from foods during eating). <https://doi.org/10.1021/bk-2000-0763>.
- Schlüter, S., Steinhart, H., Schwarz, F. J., & Kirchgessner, M. (1999). Changes in the odorants of boiled carp fillet (*Cyprinus carpio* L.) as affected by increasing methionine levels in feed. *Journal of Agricultural and Food Chemistry*, 47(12), 5146-5150. <https://doi.org/10.1021/jf9902604>.
- Shahidi, F. (1998). *Flavor of meat, meat products and seafood*. (2 ed.). Springer US (Chapter 7, Flavour of fish meat). <https://doi.org/10.1007/978-1-4615-2177-8>.
- Sun, S., Wang, S. Q., Lin, R., Cheng, S. S., Yuan, B., Wang, Z. X., & Tan, M. Q. (2020). Effect of different cooking methods on proton dynamics and physicochemical attributes in Spanish mackerel assessed by Low-Field NMR. *Foods*, 9(3), 364. <https://doi.org/10.3390/foods9030364>.
- Tao, N. P., Wang, L. Y., Gong, X., & Liu, Y. (2012). Comparison of nutritional composition of farmed pufferfish muscles among *Fugu obscurus*, *Fugu flavidus* and *Fugu rubripes*. *Journal of Food Composition and Analysis*, 28(1), 40-45. <https://doi.org/10.1016/j.jfca.2012.06.004>.
- Thomas-Danguin, T., Guichard, E., & Salles, C. (2019). Cross-modal interactions as a strategy to enhance salty taste and to maintain liking of low-salt food: a review. *Food & Function*, 10(9), 5269-5281. <https://doi.org/10.1039/c8fo02006j>.
- Tornberg, E. (2005). Effects of heat on meat proteins - Implications on structure and quality of meat products. *Meat Science*, 70(3), 493-508. <https://doi.org/10.1016/j.meatsci.2004.11.021>.
- Van Den Dool, H., & Kratz, P. D. (1963). A generalization of the retention index system including linear temperature programmed gas - liquid partition chromatography. *Journal of Chromatography A*, 11, 463-471. [https://doi.org/10.1016/S0021-9673\(01\)80947-X](https://doi.org/10.1016/S0021-9673(01)80947-X).
- Van Gemert, L. J. (2011). Odour thresholds: compilations of odour threshold values in air, water and other media, Oliemans Punter & Partners BV, Zeist, The Netherlands.
- Wang, S., Lin, R., Cheng, S., & Tan, M. (2020). Water dynamics changes and protein denaturation in surf clam evaluated by two-dimensional LF-NMR T₁-T₂ relaxation technique during heating process. *Food Chemistry*, 320, 126622. <https://doi.org/10.1016/j.foodchem.2020.126622>.
- Wang, W., Ning, M., Fan, Y., Liu, X., Chen, G., & Liu, Y. (2021). Comparison of physicochemical and umami characterization of aqueous and ethanolic Takifugu obscurus muscle extracts. *Food and Chemistry Toxicology*, 154, 112317. <https://doi.org/10.1016/j.fct.2021.112317>.
- Wang, X., Wang, X., Feng, T., Shen, Y., & Xia, S. (2021). Saltiness perception enhancement of fish meat treated by microwave: The significance of conformational characteristics, water and sodium mobility. *Food Chemistry*, 347, 129033. <https://doi.org/10.1016/j.foodchem.2021.129033>.
- Wang, W., Zhou, X., & Liu, Y. (2020). Characterization and evaluation of umami taste: A review. *TrAC Trends in Analytical Chemistry*, 127, 115876. <https://doi.org/10.1016/j.trac.2020.115876>.
- Xia, K., Wang, H., Huang, L., Xu, W., Zang, X., Song, Y. K., & Tan, M. (2017). Water dynamics in turbot (*Scophthalmus maximus*) flesh during baking and microwave heating: nuclear magnetic resonance and magnetic resonance imaging studies. *International Journal of Food Engineering*, 13(7). <https://doi.org/10.1515/ijfe-2017-0028>.
- Xu, Y., Wang, R., Zhao, H., Yin, Y., Li, X., Yi, S., & Li, J. (2020). Effect of heat treatment duration on the interaction between fish myosin and selected flavor compounds. *Journal of the Science of Food and Agriculture*, 100, 4457-4463. <https://doi.org/10.1002/jsfa.10486>.
- Yang, Y., Zhang, X., Wang, Y., Pan, D., Sun, Y., & Cao, J. (2017). Study on the volatile compounds generated from lipid oxidation of Chinese bacon (unsmoked) during processing. *European Journal of Lipid Science and Technology*, 119(10), 1600512. <https://doi.org/10.1002/ejlt.201600512>.
- Zhang, N.; Ayed, C.; Wang, W.; & Liu, Y. (2019). Sensory-guided analysis of key taste-active compounds in pufferfish (*Takifugu obscurus*). *Journal of Agricultural and Food Chemistry*, 67(50), 13809-13816. <https://doi.org/10.1021/acs.jafc.8b06047>.
- Zhang, N. L., Wang, W. L., Li, B., & Liu, Y. (2019). Non-volatile taste active compounds and umami evaluation in two aquacultured pufferfish (*Takifugu obscurus* and *Takifugu rubripes*). *Food Bioscience*, 32, 100468. <https://doi.org/10.1016/j.fbio.2019.100468>.
- Zheng, Y. Y., Zhou, C. Y., Wang, C., Ding, D. M., Wang, J.-J., Li, C. B., & Zhou, G. H. (2021). Evaluating the effect of cooking temperature and time on collagen characteristics and the texture of hog maw. *Journal of Texture Studies*, 52(2), 207-218.

<https://doi.org/10.1111/jtxs.12580>.

Zhou, C. Y., Wang, C., Cai, J.-H., Bai, Y., Yu, X. B., Li, C. B., Xu, X. L., Zhou, G. H., & Cao, J. X. (2019). Evaluating the effect of protein modifications and water distribution on bitterness and adhesiveness of Jinhua ham. *Food Chemistry*, *293*, 103-111.

<https://doi.org/10.1016/j.foodchem.2019.04.095>.

Zhou, X., & Wang, C. Y. (2017). *Dream of Fugu*. (1 ed.). Modern Press, China Publishing Group Corp., Beijing, China.

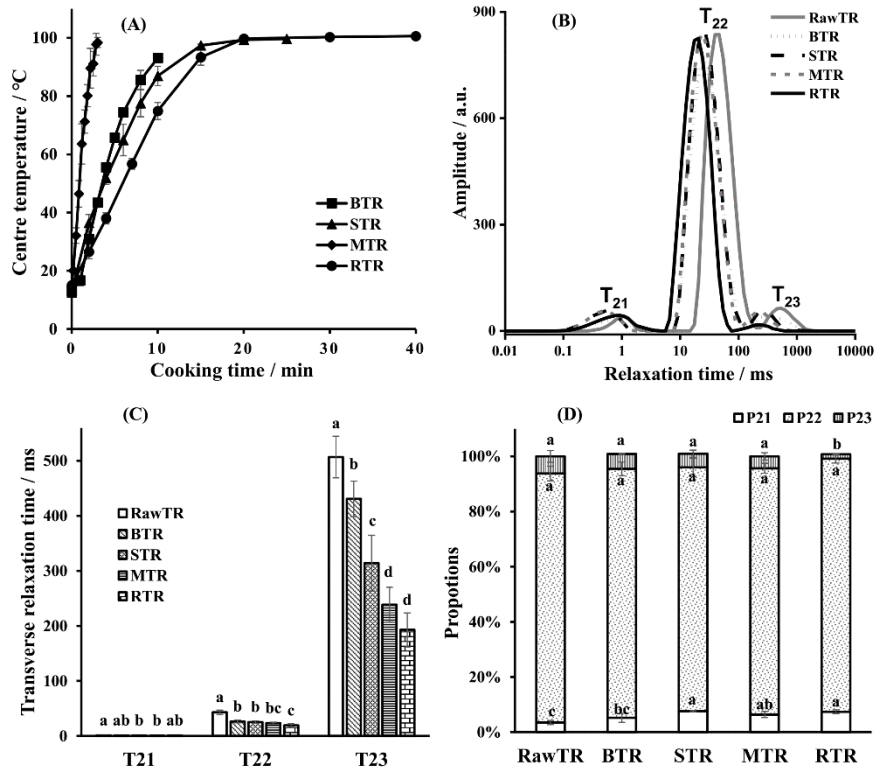


Figure 1 Centre temperature curves (A) and water dynamic of raw and cooked *T. rubripes* by LF-NMR ^{1,2}: (B) continuous transverse relaxation time curves; (C) transverse relaxation time (T₂₁, bound water, T₂₂, immobilised water, T₂₃, free water); (D) peak area proportion (P₂₁, P₂₂, P₂₃)

1. Different lowercases (a, b, c, d) of each parameter among samples indicated significant difference by ANOVA with a Post-hoc Tukey test at $\alpha=0.05$. Error bars represented standard deviations of means (n=4).
2. Abbreviations: RawTR, Raw *T. rubripes*; BTR, Boiled *T. rubripes*; STR, Steamed *T. rubripes*; MTR, Microwave-heated *T. rubripes*; RTR, Roasted *T. rubripes*.

Table 1 Water content and colour of raw and cooked *T. rubripes* ¹

Cooked <i>T. rubripes</i>	Remaining weight (%)	Moisture (%)	Colour			ΔE^2
			L*	a*	b*	
Raw <i>T. rubripes</i> (RawTR)	-	79.70 ± 0.00 a	54.91 ± 0.76 d	-1.83 ± 0.13 d	-3.90 ± 0.58 d	-
Boiled <i>T. rubripes</i> (BTR)	67.92 ± 0.02 a	70.77 ± 0.01 b	77.82 ± 1.11 b	-0.76 ± 0.34 b	8.49 ± 1.23 c	26.07
Steamed <i>T. rubripes</i> (STR)	63.14 ± 0.03 b	69.22 ± 0.01 bc	76.85 ± 1.29 b	-0.53 ± 0.14 b	10.93 ± 0.64 b	26.51
Microwave-heated <i>T. rubripes</i> (MTR)	62.87 ± 0.01 b	69.00 ± 0.02 c	80.33 ± 1.42 a	-1.11 ± 0.21 c	7.60 ± 1.30 c	27.92
Roasted <i>T. rubripes</i> (RTR)	47.80 ± 0.02 c	56.93 ± 0.02 d	65.85 ± 1.58 c	3.36 ± 0.26 a	20.92 ± 1.36 a	27.62

1. The data were presented as Mean ± Standard Deviation (n=8). Different lowercases (a, b, c, d) for each column indicated significant difference by ANOVA with a Post-hoc Tukey test at $\alpha=0.05$.
2. Reference to Raw *Takifugu rubripes* (RawTR).

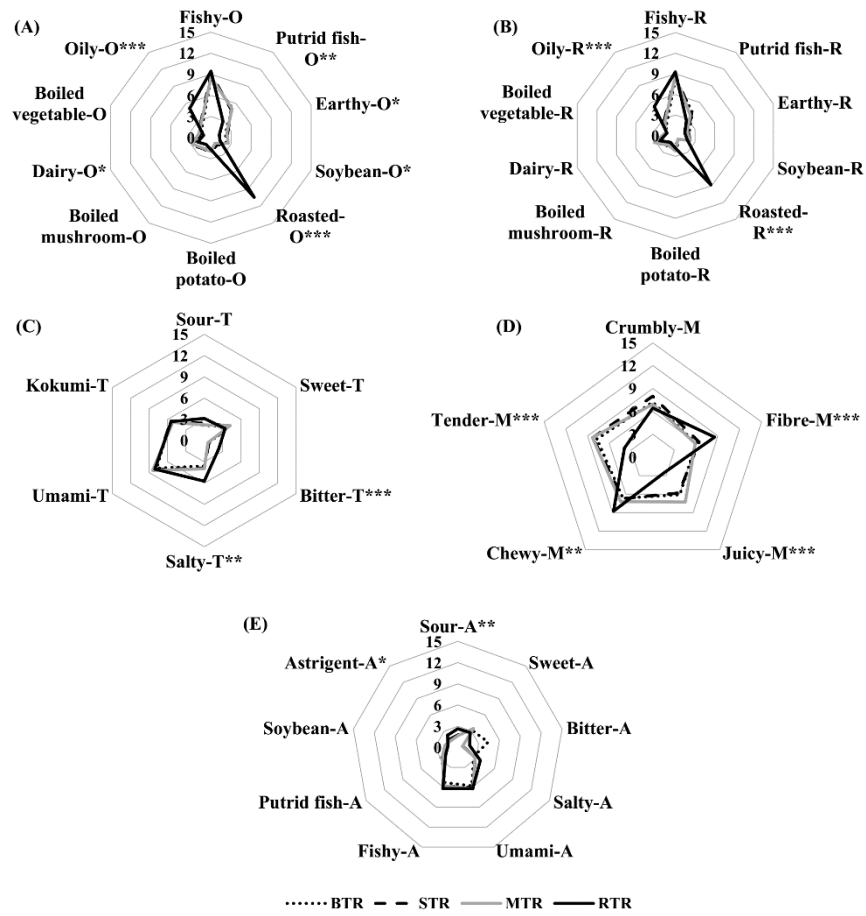


Figure 2 The quantitative descriptive analysis (QDA) results of cooked *T. rubripes*^{1,2}: profiles of (A) orthonasal aroma, (B) retronasal aroma, (C) taste, (D) mouthfeel and (E) after-effect

1. *, **, ***: significant at $p < 0.05$, $p < 0.001$ and $p < 0.0001$ respectively ($n=3$).
2. Abbreviations: BTR, Boiled *T. rubripes* (dotted lines); STR, Steamed *T. rubripes* (dashed lines); MTR, Microwave-heated *T. rubripes* (grey solid lines); RTR, Roasted *T. rubripes* (black solid lines).

(2E)

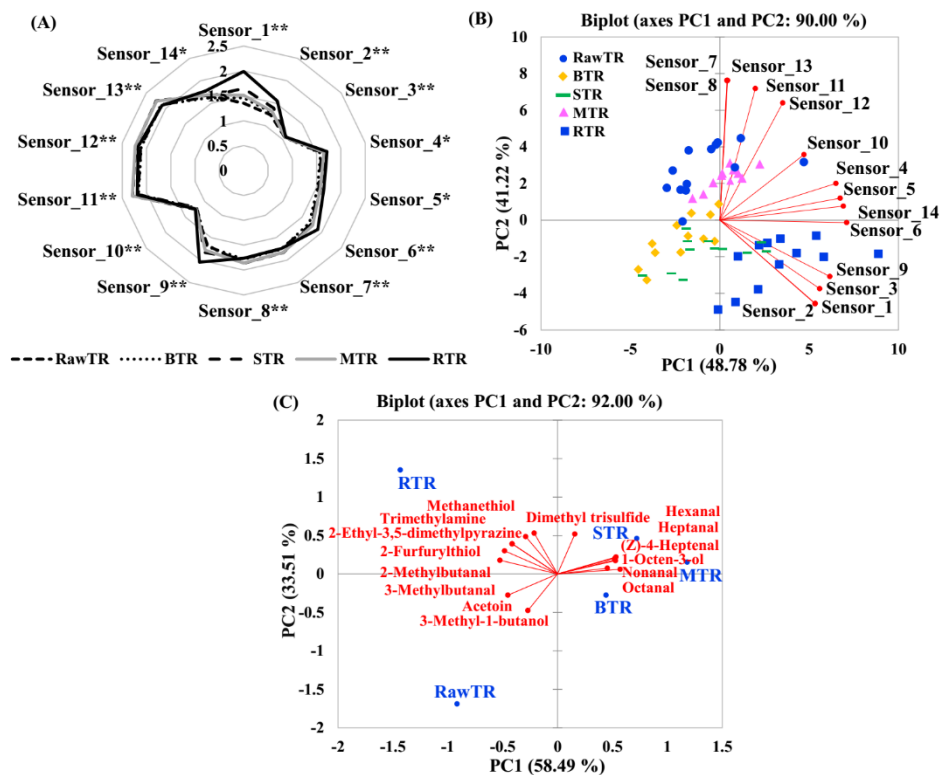


Figure 3 Aroma analysis of cooked *T. rubripes*¹ with a radar chart (A)² and Principal Component Analysis (PCA) (B) based on E-nose data and a PCA (C) from the volatile compounds with the relative odour activity value³ higher than 1 based on GC-TOFMS data and thresholds

1. Abbreviations: RawTR, Raw *T. rubripes*; BTR, Boiled *T. rubripes*; STR, Steamed *T. rubripes*; MTR, Microwave-heated *T. rubripes*; RTR, Roasted *T. rubripes*.
2. *, **: significant at $p < 0.001$ and $p < 0.0001$ respectively ($n=12$).
3. Relative odour activity value was calculated as the ratio of the relative headspace concentration to the threshold from Table 2.

Table 2 Volatile compounds and relative headspace concentration of cooked *T. rubripes*

($\mu\text{g}/\text{kg}$)¹

No.	Volatile compounds ²	CAS	Threshold ($\mu\text{g}/\text{kg}$) ³	RI ⁴	Concentration ($\mu\text{g}/\text{kg}$)				
					RawTR	BTR	STR	MTR	RTR
Hydrocarbons (36)									
1	Hexane	110-54-3	-	600	18.35 ± 6.00 b	7.19 ± 3.41 b	13.76 ± 6.22 b	82.90 ± 74.29 a	62.26 ± 11.32 ab
2	Heptane	142-82-5	50000	700	2.42 ± 0.57 b	13.54 ± 2.87 a	18.50 ± 5.87 a	14.06 ± 1.78 a	19.39 ± 5.25 a
3	Ethylcyclohexane	1678-91-7	-	885	-	0.54 ± 0.23 bc	0.83 ± 0.08 ab	0.40 ± 0.09 bc	1.24 ± 0.83 a
4	1,2,3-Trimethylcyclopentene	473-91-6	-	892	3.93 ± 2.24 a	4.32 ± 1.41 a	4.04 ± 0.42 a	4.63 ± 1.13 a	4.81 ± 2.92 a
5	Nonane	111-84-2	10000	900	0.65 ± 0.42 c	1.92 ± 0.80 b	2.72 ± 0.57 b	2.24 ± 0.60 b	4.24 ± 0.66 a
6	2,4-Octadiene	13643-08-8	-	926	1.18 ± 0.62 b	3.18 ± 1.21 a	4.64 ± 0.48 a	3.78 ± 0.82 a	4.79 ± 1.05 a
7	Benzene	71-43-2	72 d	939	1.90 ± 0.38 b	3.65 ± 1.21 a	4.51 ± 0.86 a	3.56 ± 0.53 a	4.44 ± 0.85 a
8	2,2,4,6,6-Pentamethylheptane	13475-82-6	-	961	0.85 ± 0.37 a	0.84 ± 0.21 a	1.27 ± 0.54 a	0.78 ± 0.09 a	0.67 ± 0.62 a
9	Decane	124-18-5	10000 d	1000	0.11 ± 0.06 b	0.13 ± 0.04 b	0.18 ± 0.06 b	0.16 ± 0.03 b	0.27 ± 0.05 a
10	α -Pinene	80-56-8	14 d	1014	0.96 ± 0.45 b	1.39 ± 0.20 ab	1.59 ± 0.39 a	1.67 ± 0.32 a	1.75 ± 0.24 a
11	Toluene	108-88-3	527 d	1038	6.21 ± 2.94 b	7.02 ± 1.81 ab	7.20 ± 1.01 ab	6.81 ± 1.47 ab	10.62 ± 2.67 a
12	β -Pinene	127-91-3	140 d	1093	0.54 ± 0.11 b	0.83 ± 0.14 ab	1.07 ± 0.21 a	1.26 ± 0.33 a	1.20 ± 0.22 a
13	Undecane	1120-21-4	10000	1100	0.30 ± 0.12 ab	0.20 ± 0.06 b	0.28 ± 0.05 ab	0.25 ± 0.04 b	0.41 ± 0.04 a
14	β -Phellandrene	555-10-2	500 d	1107	0.21 ± 0.12 b	1.32 ± 0.60 a	0.91 ± 0.21 a	1.19 ± 0.41 a	0.97 ± 0.18 a
15	Ethylbenzene	100-41-4	2205.25 d	1119	1.75 ± 0.77 a	2.08 ± 0.73 a	2.56 ± 0.56 a	2.09 ± 0.45 a	2.75 ± 0.69 a
16	1,4-Dimethylbenzene	106-42-3	250 d	1128	1.06 ± 0.51 a	1.34 ± 0.44 a	1.51 ± 0.31 a	1.40 ± 0.28 a	1.79 ± 0.51 a
17	1,3-Dimethylbenzene	108-38-3	1000	1134	2.30 ± 1.03 b	3.13 ± 0.76 ab	4.00 ± 0.84 ab	3.64 ± 0.90 ab	4.48 ± 1.06 a
18	3-Methylundecane	1002-43-3	-	1158	0.06 ± 0.03 ab	0.09 ± 0.03 a	0.06 ± 0.03 ab	0.03 ± 0.00 b	0.05 ± 0.01 ab
19	β -Myrcene	123-35-3	1.2 d	1156	-	0.15 ± 0.03 b	0.22 ± 0.05 ab	0.22 ± 0.06 ab	0.26 ± 0.05 a
20	D-Limonene	5989-27-5	34 d	1188	0.92 ± 0.43 c	1.36 ± 0.34 bc	3.93 ± 1.09 a	1.60 ± 0.37 bc	2.45 ± 0.75 b
21	Dodecane	112-40-3	10000 d	1200	0.36 ± 0.12 c	0.46 ± 0.06 c	0.91 ± 0.24 a	0.61 ± 0.07 bc	0.84 ± 0.12 ab
22	Propylbenzene	103-65-1	177.12 d	1203	0.06 ± 0.03 b	0.10 ± 0.03 ab	0.12 ± 0.02 ab	0.12 ± 0.03 a	0.15 ± 0.05 a
23	<i>m</i> -Ethyltoluene	620-14-4	800 r	1217	0.24 ± 0.12 c	0.40 ± 0.09 bc	0.53 ± 0.13 ab	0.52 ± 0.10 ab	0.71 ± 0.20 a
24	<i>p</i> -Ethyltoluene	622-96-8	600 r	1220	1.22 ± 0.75 a	1.42 ± 0.43 a	1.51 ± 0.33 a	1.48 ± 0.27 a	1.86 ± 0.50 a
25	Mesitylene	108-67-8	3 d	1239	0.61 ± 0.30 a	0.73 ± 0.16 a	0.76 ± 0.12 a	0.74 ± 0.11 a	0.90 ± 0.30 a
26	Styrene	100-42-5	3.6 d	1257	0.55 ± 0.26 a	0.68 ± 0.24 a	0.67 ± 0.17 a	0.60 ± 0.12 a	0.80 ± 0.21 a
27	<i>p</i> -Cymene	99-87-6	6.2 d	1264	0.38 ± 0.16 b	0.54 ± 0.16 ab	0.76 ± 0.14 a	0.73 ± 0.21 a	0.85 ± 0.17 a
28	Pseudocumene	95-63-6	260 r	1278	0.92 ± 0.43 b	1.55 ± 0.37 ab	1.65 ± 0.30 ab	1.63 ± 0.24 ab	2.03 ± 0.57 a
29	Tridecane	629-50-5	-	1300	0.36 ± 0.08 d	0.69 ± 0.13 c	1.09 ± 0.24 ab	0.83 ± 0.07 bc	1.25 ± 0.21 a
30	4-Propyltoluene	1074-55-1	-	1299	0.26 ± 0.11 c	0.45 ± 0.07 b	0.69 ± 0.10 a	0.56 ± 0.11 ab	0.74 ± 0.08 a
31	2-Ethyl- <i>p</i> -xylene	1758-88-9	-	1321	0.18 ± 0.09 b	0.36 ± 0.10 ab	0.36 ± 0.06 ab	0.36 ± 0.05 ab	0.46 ± 0.12 a
32	1,2,3-Trimethylbenzene	526-73-8	-	1334	0.92 ± 0.35 a	0.94 ± 0.24 a	0.94 ± 0.10 a	0.94 ± 0.11 a	1.07 ± 0.31 a
33	Tetradecane	629-59-4	1	1400	0.37 ± 0.10 b	0.36 ± 0.06 b	0.56 ± 0.08 a	0.42 ± 0.03 ab	0.51 ± 0.12 ab
34	2,5-Dimethyl- <i>p</i> -xylene	95-93-2	-	1433	0.21 ± 0.08 b	0.39 ± 0.11 a	0.40 ± 0.05 a	0.38 ± 0.04 a	0.46 ± 0.11 a
35	Pentadecane	629-62-9	-	1500	-	-	0.05 ± 0.00 b	0.04 ± 0.00 b	0.08 ± 0.02 a
36	2,6,10,14-Tetramethylpentadecane	1921-70-6	-	1679	0.06 ± 0.02 c	0.08 ± 0.02 bc	0.13 ± 0.01 b	0.08 ± 0.01 bc	0.20 ± 0.06 a
Sulphur-containing compounds (11)									
37	Methanethiol	74-93-1	0.02 d	681	-	12.38 ± 2.96 cd	36.07 ± 4.31 b	18.15 ± 6.92 c	66.87 ± 18.91 a
38	Dimethyl disulfide	624-92-0	1.1 d	1071	-	0.98 ± 0.27 a	0.76 ± 0.19 ab	0.55 ± 0.14 b	0.56 ± 0.22 b
39	3-Methylthiophene	616-44-4	-	1089	-	-	0.18 ± 0.02 b	-	0.75 ± 0.18 a
40	2-Ethylthiophene	872-55-9	-	1168	0.19 ± 0.10 b	0.22 ± 0.07 b	0.37 ± 0.08 b	0.19 ± 0.03 b	0.57 ± 0.17 a
41	4-Methylthiazole	693-95-8	55 d	1288	-	-	-	-	0.16 ± 0.04 a
42	Dimethyl trisulfide	3658-80-8	0.1 d	1376	-	0.15 ± 0.03 b	0.27 ± 0.07 a	0.16 ± 0.07 b	0.23 ± 0.06 ab
43	2-Furfurylthiol	98-02-2	0.036 d	1438	-	-	-	-	0.24 ± 0.06 a
44	Methional	3268-49-3	0.45 d	1464	-	-	-	-	0.14 ± 0.04 a
45	2-Acetylthiazole	24295-03-2	3 d	1656	-	-	-	-	0.12 ± 0.02 a
46	5-Methyl-2-thiophenecarboxaldehyde	13679-70-4	-	1737	-	-	0.04 ± 0.01 b	-	0.13 ± 0.01 a
47	Benzothiazole	95-16-9	80 d	1966	0.35 ± 0.15 a	0.31 ± 0.06 a	0.24 ± 0.07 a	0.34 ± 0.08 a	0.26 ± 0.08 a
Nitrogen-containing compounds (15)									
48	Trimethylamine	75-50-3	8 d	827	36.67 ± 9.94 c	44.45 ± 11.25 c	94.75 ± 21.81 b	49.82 ± 11.49 c	160.06 ± 24.82 a
49	Methylpyrazine	109-08-0	30000 d	1275	-	0.26 ± 0.06 b	0.10 ± 0.03 b	0.04 ± 0.01 b	5.49 ± 0.89 a
50	2-Ethyl-pyridine	100-71-0	-	1290	-	-	0.21 ± 0.04 ab	0.16 ± 0.03 b	0.22 ± 0.04 a
51	2,5-Dimethylpyrazine	123-32-0	1750 d	1332	-	0.11 ± 0.03 b	0.08 ± 0.01 b	0.12 ± 0.02 b	3.07 ± 0.34 a
52	2,6-Dimethylpyrazine	108-50-9	718 d	1338	-	0.08 ± 0.02 b	0.09 ± 0.02 b	0.12 ± 0.04 b	3.30 ± 0.50 a

53	2,3-Dimethylpyrazine	5910-89-4	800 d	1356	-	-	-	-	1.18 ± 0.18 a
54	2-Ethyl-5-methylpyrazine	13360-64-0	16 d	1392	-	0.12 ± 0.04 bc	0.12 ± 0.03 bc	0.19 ± 0.02 b	1.45 ± 0.22 a
55	2-Ethyl-6-methylpyrazine	13925-03-6	40 d	1398	-	-	-	-	0.87 ± 0.09 a
56	Trimethylpyrazine	14667-55-1	350.12 d	1414	-	-	-	-	4.82 ± 0.10 a
57	2,6-Diethylpyrazine	13067-27-1	6 d	1439	-	-	-	-	0.11 ± 0.02 a
58	3-Ethyl-2,5-dimethylpyrazine	13360-65-1	8.6 d	1452	-	-	-	-	1.40 ± 0.39 a
59	2-Ethyl-3,5-dimethylpyrazine	13925-07-0	0.04 d	1468	-	-	-	-	1.25 ± 0.16 a
60	Tetramethylpyrazine	1124-11-4	2525.02 d	1484	-	-	-	-	0.32 ± 0.00 a
61	2,3,5-Trimethyl-6-ethylpyrazine	17398-16-2	-	1520	-	-	-	-	0.19 ± 0.03 a
62	Pyrrrole	109-97-7	20000 d	1523	-	0.16 ± 0.01 b	0.14 ± 0.03 b	0.11 ± 0.04 b	0.92 ± 0.32 a
Aldehydes (12)									
63	2-Methylbutanal	96-17-3	1 d	916	8.11 ± 3.69 b	6.81 ± 4.12 b	6.57 ± 0.62 b	6.62 ± 1.40 b	13.92 ± 3.04 a
64	3-Methylbutanal	590-86-3	1.1 d	920	19.75 ± 7.80 b	5.14 ± 2.41 c	6.61 ± 0.82 c	8.28 ± 0.77 c	35.66 ± 5.60 a
65	Pentanal	110-62-3	12 d	983	4.08 ± 0.96 b	10.22 ± 2.84 a	11.76 ± 1.51 a	11.57 ± 3.17 a	5.95 ± 1.24 b
66	Hexanal	66-25-1	5 d	1083	24.11 ± 8.22 b	52.99 ± 13.00 a	59.70 ± 6.94 a	65.71 ± 8.46 a	35.11 ± 7.63 b
67	Heptanal	111-71-7	2.8 d	1186	4.39 ± 0.92 b	6.46 ± 2.02 ab	8.16 ± 2.01 a	7.52 ± 2.10 ab	4.80 ± 1.02 ab
68	(Z)-4-Heptenal	6728-31-0	0.0087 d	1244	0.62 ± 0.18 c	1.15 ± 0.37 abc	1.28 ± 0.21 ab	1.60 ± 0.43 a	0.84 ± 0.19 bc
69	Octanal	124-13-0	0.587 d	1291	2.62 ± 0.31 b	3.50 ± 0.77 ab	4.03 ± 1.00 a	4.25 ± 0.83 a	2.41 ± 0.54 b
70	Nonanal	124-19-6	1.1 d	1396	1.52 ± 0.26 b	1.74 ± 0.36 b	1.97 ± 0.38 b	3.05 ± 0.63 a	1.50 ± 0.17 b
71	Furfural	98-01-1	9562 d	1476	-	-	-	-	0.45 ± 0.17 a
72	(E)-2-Octenal	2548-87-0	3 d	1494	0.23 ± 0.04 ab	0.22 ± 0.08 ab	0.30 ± 0.05 a	0.25 ± 0.06 ab	0.17 ± 0.03 b
73	Benzaldehyde	100-52-7	750.89 d	1532	1.44 ± 0.63 b	1.65 ± 0.19 b	2.60 ± 0.60 ab	2.05 ± 0.51 b	3.67 ± 0.91 a
74	4-Ethylbenzaldehyde	53951-50-1	-	1716	0.24 ± 0.06 b	0.39 ± 0.08 ab	0.50 ± 0.13 a	0.51 ± 0.15 a	0.35 ± 0.08 ab
Ketones (15)									
75	2-Butanone	78-93-3	35400.2 d	908	3.07 ± 0.46 b	3.32 ± 0.38 b	4.01 ± 1.03 b	3.70 ± 0.69 b	6.58 ± 1.74 a
76	2,3-Pentanedione	600-14-6	20 d	1065	2.49 ± 0.62 b	3.46 ± 0.96 ab	3.87 ± 0.74 ab	4.39 ± 1.32 a	2.25 ± 0.44 b
77	6-Methyl-2-heptanone	928-68-7	8.1 d	1240	0.51 ± 0.22 a	0.38 ± 0.13 a	0.41 ± 0.06 a	0.37 ± 0.05 a	0.30 ± 0.10 a
78	Dihydro-2-methyl-3(2H)-furanone	3188-00-9	-	1270	-	-	-	-	0.38 ± 0.12 a
79	Acetoin	513-86-0	14 d	1296	20.09 ± 6.45 a	2.60 ± 0.55 c	6.72 ± 1.28 bc	2.80 ± 0.79 c	11.52 ± 2.45 b
80	1-Hydroxy-2-propanone	116-09-6	80000 d	1313	-	1.31 ± 0.15 c	8.25 ± 1.86 b	1.49 ± 0.37 c	42.16 ± 6.81 a
81	(Z)-6-Octen-2-one	74810-53-0	-	1336	0.26 ± 0.09 b	0.76 ± 0.31 a	0.68 ± 0.10 a	0.78 ± 0.24 a	0.44 ± 0.11 ab
82	6-Methyl-5-hepten-2-one	110-93-0	68 d	1342	0.25 ± 0.09 a	0.31 ± 0.13 a	0.38 ± 0.03 a	0.41 ± 0.09 a	0.43 ± 0.12 a
83	2-Hydroxy-3-pentanone	5704-20-1	-	1368	-	0.33 ± 0.06 b	0.48 ± 0.11 a	0.54 ± 0.07 a	0.49 ± 0.09 a
84	2-Nonanone	821-55-6	41 d	1393	3.21 ± 0.78 b	2.01 ± 0.30 c	2.94 ± 0.22 bc	4.10 ± 0.70 a	2.29 ± 0.28 bc
85	1-(Acetyloxy)-2-propanone	592-20-1	-	1480	-	-	-	-	4.73 ± 1.24 a
86	3,5-Octadienone	38284-27-4	-	1530	1.31 ± 0.13 ab	1.25 ± 0.29 ab	1.41 ± 0.33 ab	1.74 ± 0.36 a	0.97 ± 0.26 b
87	2-Undecanone	112-12-9	5.5 d	1604	0.18 ± 0.03 a	0.12 ± 0.04 a	0.18 ± 0.03 a	0.20 ± 0.05 a	0.15 ± 0.03 a
88	Butyrolactone	96-48-0	20000	1644	0.40 ± 0.14 b	0.28 ± 0.09 b	0.34 ± 0.03 b	0.29 ± 0.06 b	1.34 ± 0.46 a
89	4-Hydroxy-5-methyl-3(2H)-furanone	19322-27-1	2100 d	2144	-	0.08 ± 0.01 b	0.36 ± 0.10 b	0.07 ± 0.00 b	1.58 ± 0.38 a
Alcohols (18)									
90	1-Propanol	71-23-8	8505.6 d	1046	0.70 ± 0.16 a	0.82 ± 0.21 a	1.06 ± 0.29 a	1.09 ± 0.31 a	0.76 ± 0.15 a
91	1-Butanol	71-36-3	459.2 d	1156	1.27 ± 0.47 a	0.77 ± 0.20 a	0.82 ± 0.22 a	0.74 ± 0.15 a	0.77 ± 0.12 a
92	1-Penten-3-ol	616-25-1	358.1 d	1170	65.83 ± 17.77 b	111.97 ± 18.46 a	121.01 ± 15.23 a	146.94 ± 27.09 a	74.77 ± 15.60 b
93	Eucalyptol	470-82-6	1.1 d	1202	0.47 ± 0.19 b	0.47 ± 0.09 b	0.56 ± 0.07 b	0.99 ± 0.24 a	0.51 ± 0.16 b
94	3-Methyl-1-butanol	123-51-3	4 d	1217	6.00 ± 2.59 a	0.91 ± 0.27 b	0.95 ± 0.20 b	1.33 ± 0.26 b	1.23 ± 0.40 b
95	1-Pentanol	71-41-0	150.2 d	1260	1.60 ± 0.48 ab	2.17 ± 0.65 ab	2.40 ± 0.59 a	2.51 ± 0.63 a	1.26 ± 0.26 b
96	(E)-2-Penten-1-ol	1576-96-1	89.2 d	1323	0.22 ± 0.09 b	0.30 ± 0.07 ab	0.32 ± 0.03 ab	0.40 ± 0.11 a	0.24 ± 0.05 b
97	(Z)-2-Penten-1-ol	1576-95-0	720 d	1331	1.30 ± 0.45 b	1.92 ± 0.53 ab	2.10 ± 0.29 a	2.24 ± 0.13 a	1.62 ± 0.31 ab
98	1-Hexanol	111-27-3	5.6 d	1362	2.73 ± 0.47 a	1.20 ± 0.35 b	1.39 ± 0.32 b	1.59 ± 0.50 b	1.08 ± 0.29 b
99	3-Hexen-1-ol	544-12-7	1630 d	1373	0.12 ± 0.06 a	0.13 ± 0.05 a	0.16 ± 0.04 a	0.17 ± 0.04 a	0.13 ± 0.03 a
100	1-Octen-3-ol	3391-86-4	1.5 d	1460	6.12 ± 1.10 c	8.53 ± 1.71 bc	10.39 ± 1.16 ab	12.26 ± 2.73 a	7.06 ± 1.64 bc
101	1-Heptanol	111-70-6	5.4 d	1465	2.79 ± 0.65 ab	3.39 ± 0.96 ab	3.68 ± 0.96 ab	4.43 ± 1.50 a	2.20 ± 0.60 b
102	2-Ethyl-1-hexanol	104-76-7	25482.2 d	1499	0.82 ± 0.36 a	0.60 ± 0.18 a	0.56 ± 0.11 a	0.62 ± 0.09 a	0.66 ± 0.16 a
103	1-Octanol	111-87-5	125.8 d	1568	0.59 ± 0.25 a	0.28 ± 0.04 b	0.33 ± 0.08 ab	0.43 ± 0.07 ab	0.27 ± 0.04 b
104	(E)-2-Octen-1-ol	18409-17-1	40 d	1627	0.17 ± 0.03 c	0.21 ± 0.04 bc	0.30 ± 0.08 ab	0.32 ± 0.06 a	0.20 ± 0.06 bc
105	1-Nonanol	143-08-8	45.5 d	1670	0.19 ± 0.08 a	-	0.07 ± 0.01 b	0.08 ± 0.01 b	0.05 ± 0.02 b
106	2-Furanmethanol	98-00-0	4500 d	1677	-	-	-	-	2.55 ± 1.26 a
107	2,7-Octadien-1-ol	23578-51-0	-	1696	0.66 ± 0.14 c	1.18 ± 0.28 ab	1.25 ± 0.20 ab	1.54 ± 0.35 a	0.86 ± 0.20 bc
Others (10)									
108	Methyl ethanoate	79-20-9	1500 d	831	2.76 ± 1.22 a	0.21 ± 0.04 c	0.37 ± 0.07 c	0.22 ± 0.04 c	1.73 ± 0.25 b
109	2-Ethylfuran	3208-16-0	-	952	8.34 ± 1.43 b	17.27 ± 4.03 a	20.60 ± 4.05 a	21.14 ± 4.27 a	19.99 ± 4.15 a
110	Methyl butanoate	623-42-7	59 d	989	0.85 ± 0.33 a	0.34 ± 0.08 b	0.33 ± 0.06 b	0.31 ± 0.02 b	0.41 ± 0.12 b
111	2-Pentylfuran	3777-69-3	5.8 d	1228	0.60 ± 0.10 b	1.53 ± 0.39 a	2.32 ± 0.79 a	1.76 ± 0.42 a	2.34 ± 0.36 a

112	(E)-2-(2-Pentenyl)furan	70424-14-5	-	1301	0.17 ± 0.05 c	0.24 ± 0.05 bc	0.32 ± 0.05 ab	0.29 ± 0.06 ab	0.40 ± 0.07 a
113	Methyl 2-hydroxypropanoate	2155-30-8	-	1330	1.94 ± 0.85 a	0.62 ± 0.12 b	0.96 ± 0.24 b	0.90 ± 0.21 b	1.64 ± 0.24 a
114	2-Acetylfuran	1192-62-7	15025.2 d	1516	-	-	-	-	1.94 ± 0.15 a
115	3-Methylbutanoic acid	503-74-2	490 d	1689	0.76 ± 0.56 a	-	0.34 ± 0.01 b	0.31 ± 0.12 b	0.33 ± 0.05 b
116	Octanoic acid	124-07-2	3000 d	2080	1.62 ± 1.03 a	0.44 ± 0.14 b	0.19 ± 0.03 b	0.24 ± 0.09 b	0.17 ± 0.04 b
117	Nonanoic acid	112-05-0	4600	2185	0.64 ± 0.35 a	0.70 ± 0.13 a	0.23 ± 0.03 b	0.45 ± 0.27 ab	0.17 ± 0.03 b

1. The data was were presented as Mean ± Standard Error (n=4). Different lowercases for each row indicated significant differences by ANOVA with a Post-hoc Tukey test at $\alpha=0.05$.
2. Important volatile compounds, whose relative odour activity values (OAV, concentration in ppb/odour threshold) were higher than the reference thresholds, were marked in bold.
3. Thresholds were collected by previous reports (van Gemert, 2011).
4. RIs were compared with NIST Chemistry Webbook: webbook.nist.gov/chemistry/
5. Abbreviations: RawTR, Raw *T. rubripes*; BTR, Boiled *T. rubripes*; STR, Steamed *T. rubripes*; MTR, Microwave-heated *T. rubripes*; RTR, Roasted *T. rubripes*.

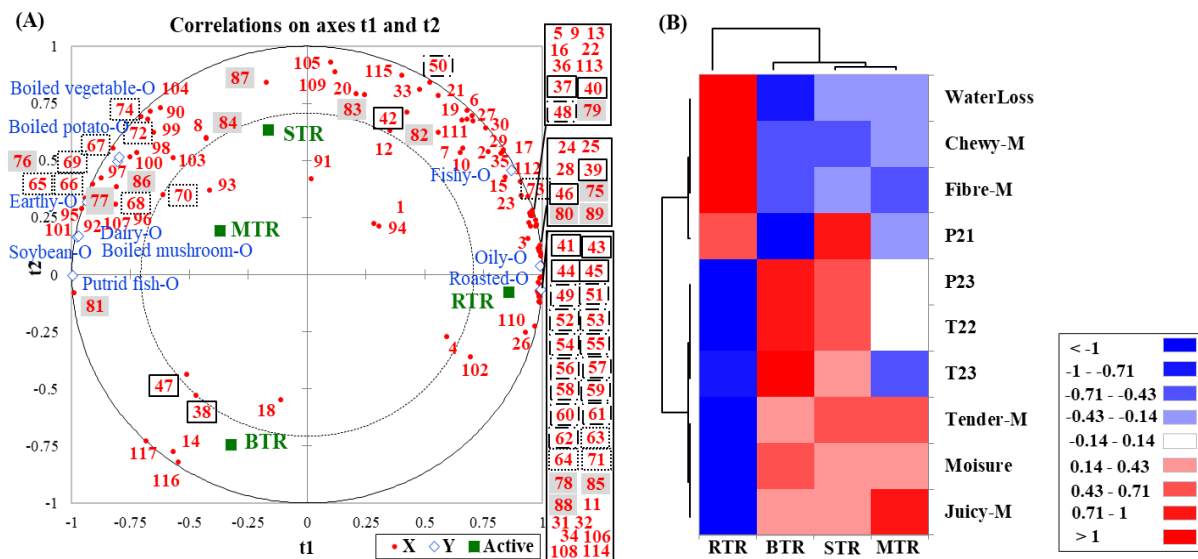


Figure 4 Correlation analysis between sensory attributes and physical-chemical properties of cooked *T. rubripes*¹: (A) Partial Least Squares Regression (PLS-R) analysis from the data of sensory orthonasal attributes and volatile compounds by GC-TOFMS^{2,3}, (B) Hierarchical Cluster Analysis Heatmap (HCA Heatmap) based on the data of water properties and sensory mouthfeel attributes with significant differences among cooked samples⁴

1. Abbreviations: BTR, Boiled *T. rubripes*; STR, Steamed *T. rubripes*; MTR, Microwave-heated *T. rubripes*; RTR, Roasted *T. rubripes*.
2. The first two components: Q^2 cum= 0.846, R^2Y cum=0.956, R^2X cum= 0.874.
3. Volatile compounds corresponded to Table 2: Sulphur-containing compounds (*solid lines*); Nitrogen-containing compounds (*dashed and solid lines*); Aldehydes (*dashed lines*); Ketones (*grey backgrounds*).
4. Red colour represented higher abundance, white represents medium abundance, and blue represented lower abundance.

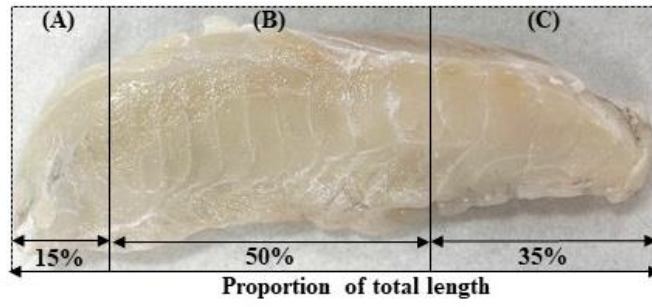


Figure S1 Sampling parts for various analysis of *T. rubripes* fillets: (A) colour and moisture analysis, (B) aroma analysis, and (C) water distribution analysis

Table S1 Sensory attributes and their definition developed by trained panellists

Attributes	Definitions	Reference	Anchors
Fishy	Pleasant aroma associated with fish	5 g Grilled cod fillet (MR.BEAVER'S, China)	nil to extreme
Putrid fish	Unpleasant aroma associated with putrid fish	5 g raw pufferfish at room temperature for 1 h (Tianzheng, China)	nil to extreme
Earthy	Aroma associated with wet soil after rain		nil to extreme
Soybean	Beany aroma associate with soybean products, such as tofu	5 g tofu (Zuming, China)	nil to extreme
Roasted	Aroma associated with roasted peanut, bread, coca powder	5 g roasted Mankattan wheat bread (200 °C, 5 min) (Mankattan, China)	nil to extreme
Boiled potato	Sweet aroma associated with boiled potato	5 g boiled potato (Wumart, China)	nil to extreme
Boiled mushroom	Aroma associated with boiled mushroom	5 g boiled mushroom (Wumart, China)	nil to extreme
Dairy	Sweet odour associated with dairy, such as milk	5 mL SATINE pure milk (Yili, China)	nil to extreme
Boiled vegetable	Aroma associated with boiled green vegetable, such as lettuces	5 g boiled lettuces (Wumart, China)	nil to extreme
Oily	Aroma associated with refined olive oil	5 mL Olivoilà olive oil (Olivoilà, China)	nil to extreme
Sour	Taste associated with organic acid	0.430 mg/mL citric acid	nil to extreme
Sweet	Taste associated with sucrose	5.76 mg/mL sucrose	nil to extreme
Bitter	Taste associated with quinine	0.0325 mg/mL quinine sulphate	nil to extreme
Salty	Taste associated with sodium chloride	1.19 mg/mL sodium chloride	nil to extreme
Umami	Taste associated with sodium glutamate	0.595 mg/mL monosodium glutamate	nil to extreme
Kokumi	Mouth-filling taste associated with chicken broth with glutathione	5.0 mM glutathione	nil to extreme
Crumbly	Easily break the sample into pieces during chewing		regular to irregular
Fibre	Muscle fibre sense of the sample when chewing		nil to extreme
Juicy	Moisture released in the early stage of chewing		nil to extreme
Chewy	Number of chewing times until swallowing		nil to extreme
Tender	Minimum force required to chew samples		higher force to lower force
Astringent	Dryness mouthfeel sensation such as the contraction of the oral mucous surface		nil to extreme

Table S2 Water distribution of cooked *T. rubripes*¹ by LF-NMR

Cooked <i>T. rubripes</i>	Relaxation time/ms			Proportions/%		
	T21	T22	T23	P21	P22	P23
Raw <i>T. rubripes</i> (RawTR)	1.03 ± 0.22 a	42.93 ± 4.03 a	506.94 ± 37.80 a	3.48 ± 0.01 c	90.33 ± 0.03 a	6.19 ± 0.02 a
Boiled <i>T. rubripes</i> (BTR)	0.73 ± 0.19 ab	26.34 ± 2.47 b	430.78 ± 32.12 b	5.16 ± 0.02 bc	90.30 ± 0.02 a	5.45 ± 0.00 a
Steamed <i>T. rubripes</i> (STR)	0.58 ± 0.12 b	25.27 ± 2.14 b	313.96 ± 50.49 c	7.59 ± 0.00 a	88.45 ± 0.03 a	4.96 ± 0.01 a
Microwave-heated <i>T. rubripes</i> (MTR)	0.52 ± 0.09 b	23.29 ± 1.82 bc	238.54 ± 31.61 d	6.41 ± 0.01 ab	89.30 ± 0.02 a	4.29 ± 0.01 a
Roasted <i>T. rubripes</i> (RTR)	0.74 ± 0.23 ab	19.16 ± 3.36 c	192.64 ± 30.98 d	7.39 ± 0.01 a	91.80 ± 0.02 a	1.58 ± 0.00 b

1. The data were presented as Mean ± Standard Deviation. Different lowercases (a, b, c) for each column indicate significant difference by ANOVA with a Post-hoc Tukey test at $\alpha=0.05$ (n=4).

Table S3 Perceived intensities of sensory attributes of cooked *T. rubripes* ^{1,2}

No.		Boiled <i>T. rubripes</i> (BTR)	Steamed <i>T. rubripes</i> (STR)	Microwave-heated <i>T. rubripes</i> (MTR)	Roasted <i>T. rubripes</i> (RTR)
<u><i>Orthonasal/Rethonasal</i></u>					
<u><i>aroma (O/R)</i></u>					
1	Fishy-O	8.44 ± 0.56 a	9.11 ± 0.55 a	8.58 ± 0.64 a	9.46 ± 0.69 a
2	Fishy-R	8.27 ± 0.86 a	8.77 ± 0.66 a	8.70 ± 0.80 a	9.29 ± 0.77 a
3	Putrid fish-O	5.17 ± 0.94 a	4.91 ± 0.84 a	5.09 ± 0.82 a	2.92 ± 0.82 b
4	Putrid fish-R	4.23 ± 0.86 a	4.03 ± 0.86 a	3.71 ± 0.84 a	2.74 ± 0.76 a
5	Earthy-O	2.19 ± 0.58 ab	2.52 ± 0.60 a	2.37 ± 0.58 a	1.23 ± 0.31 b
6	Earthy-R	2.15 ± 0.53 a	1.97 ± 0.51 a	1.80 ± 0.45 a	1.44 ± 0.37 a
7	Soybean-O	2.26 ± 0.51 ab	2.30 ± 0.51 ab	2.57 ± 0.54 a	1.36 ± 0.35 b
8	Soybean-R	2.12 ± 0.47 a	2.28 ± 0.46 a	2.26 ± 0.48 a	1.82 ± 0.39 a
9	Roasted-O	1.03 ± 0.43 b	1.34 ± 0.49 b	0.99 ± 0.28 b	10.46 ± 0.65 a
10	Roasted-R	0.65 ± 0.20 b	1.14 ± 0.55 b	0.62 ± 0.21 b	8.83 ± 1.03 a
11	Boiled potato-O	1.91 ± 0.39 a	2.10 ± 0.41 a	1.96 ± 0.30 a	1.70 ± 0.48 a
12	Boiled potato-R	1.64 ± 0.34 a	1.74 ± 0.37 a	2.20 ± 0.46 a	1.79 ± 0.46 a
13	Boiled mushroom-O	1.85 ± 0.45 a	1.92 ± 0.43 a	1.87 ± 0.34 a	1.20 ± 0.32 a
14	Boiled mushroom-R	1.84 ± 0.37 a	1.68 ± 0.39 a	1.70 ± 0.37 a	1.20 ± 0.32 a
15	Dairy-O	2.85 ± 0.49 ab	3.14 ± 0.50 a	2.84 ± 0.53 ab	1.98 ± 0.36 b
16	Dairy-R	3.16 ± 0.48 a	2.76 ± 0.46 a	3.20 ± 0.55 a	2.36 ± 0.43 a
17	Boiled vegetable-O	1.35 ± 0.47 a	1.62 ± 0.62 a	1.80 ± 0.63 a	1.11 ± 0.38 a
18	Boiled vegetable-R	1.46 ± 0.58 a	1.38 ± 0.57 a	1.46 ± 0.59 a	1.27 ± 0.47 a
19	Oily-O	2.08 ± 0.29 b	2.51 ± 0.33 b	2.39 ± 0.39 b	5.15 ± 0.71 a
20	Oily-R	2.15 ± 0.32 b	2.76 ± 0.43 b	2.57 ± 0.35 b	5.21 ± 0.65 a
<u><i>Taste (T)</i></u>					
1	Sour-T	2.18 ± 0.49 a	2.44 ± 0.40 a	2.23 ± 0.45 a	3.13 ± 0.66 a
2	Sweet-T	3.94 ± 0.74 a	4.10 ± 0.82 a	4.22 ± 0.78 a	3.41 ± 0.71 a
3	Bitter-T	0.70 ± 0.22 b	0.76 ± 0.21 b	0.59 ± 0.20 b	2.35 ± 0.55 a
4	Salty-T	3.59 ± 0.66 b	3.88 ± 0.68 b	3.98 ± 0.73 b	5.74 ± 0.65 a
5	Umami-T	7.80 ± 0.87 a	8.13 ± 0.73 a	8.43 ± 0.85 a	8.07 ± 0.73 a
6	Kokumi-T	5.43 ± 0.81 a	5.46 ± 0.81 a	5.17 ± 0.79 a	5.39 ± 0.87 a
<u><i>Mouthfeel (M)</i></u>					
1	Crumbly-M	7.23 ± 0.96 a	7.99 ± 0.86 a	6.95 ± 0.95 a	6.44 ± 0.95 a
2	Fibre-M	5.96 ± 0.78 b	6.40 ± 0.83 b	5.87 ± 0.81 b	8.53 ± 0.86 a
3	Juicy-M	6.06 ± 0.71 ab	5.80 ± 0.69 b	7.27 ± 0.87 a	2.52 ± 0.49 c
4	Chewy-M	6.64 ± 0.74 b	6.72 ± 0.75 b	7.17 ± 0.78 b	8.75 ± 0.78 a
5	Tender-M	7.71 ± 0.95 a	8.26 ± 0.89 a	8.31 ± 0.81 a	3.92 ± 0.59 b
<u><i>After-effect (A)</i></u>					
1	Sour-A	1.71 ± 0.33 b	1.75 ± 0.34 b	1.63 ± 0.32 b	2.64 ± 0.55 a
2	Sweet-A	3.18 ± 0.69 a	3.29 ± 0.69 a	3.47 ± 0.59 a	2.72 ± 0.60 a
3	Bitter-A	4.35 ± 6.27 a	0.73 ± 0.23 a	0.65 ± 0.24 a	1.69 ± 0.44 a
4	Salty-A	2.59 ± 0.55 a	2.88 ± 0.54 a	2.84 ± 0.52 a	3.68 ± 0.48 a
5	Umami-A	5.79 ± 0.86 a	6.05 ± 0.88 a	6.24 ± 0.88 a	6.22 ± 0.82 a
6	Fishy-A	5.29 ± 0.83 a	5.82 ± 0.81 a	5.78 ± 0.84 a	6.18 ± 0.89 a
7	Putrid fish-A	2.65 ± 0.71 a	2.37 ± 0.61 a	2.51 ± 0.64 a	1.96 ± 0.59 a
8	Soybean-A	1.62 ± 0.46 a	1.63 ± 0.38 a	1.85 ± 0.46 a	1.40 ± 0.37 a
9	Astringent-A	1.51 ± 0.34 b	1.61 ± 0.32 ab	1.36 ± 0.24 b	2.25 ± 0.47 a

1. The data were presented as Mean ± Standard Error (n=3). Different lowercases (a, b, c) for each row indicated significant difference by ANOVA with a Post-hoc Tukey test at $\alpha=0.05$.
2. Attributes with significant differences were highlighted in bold.